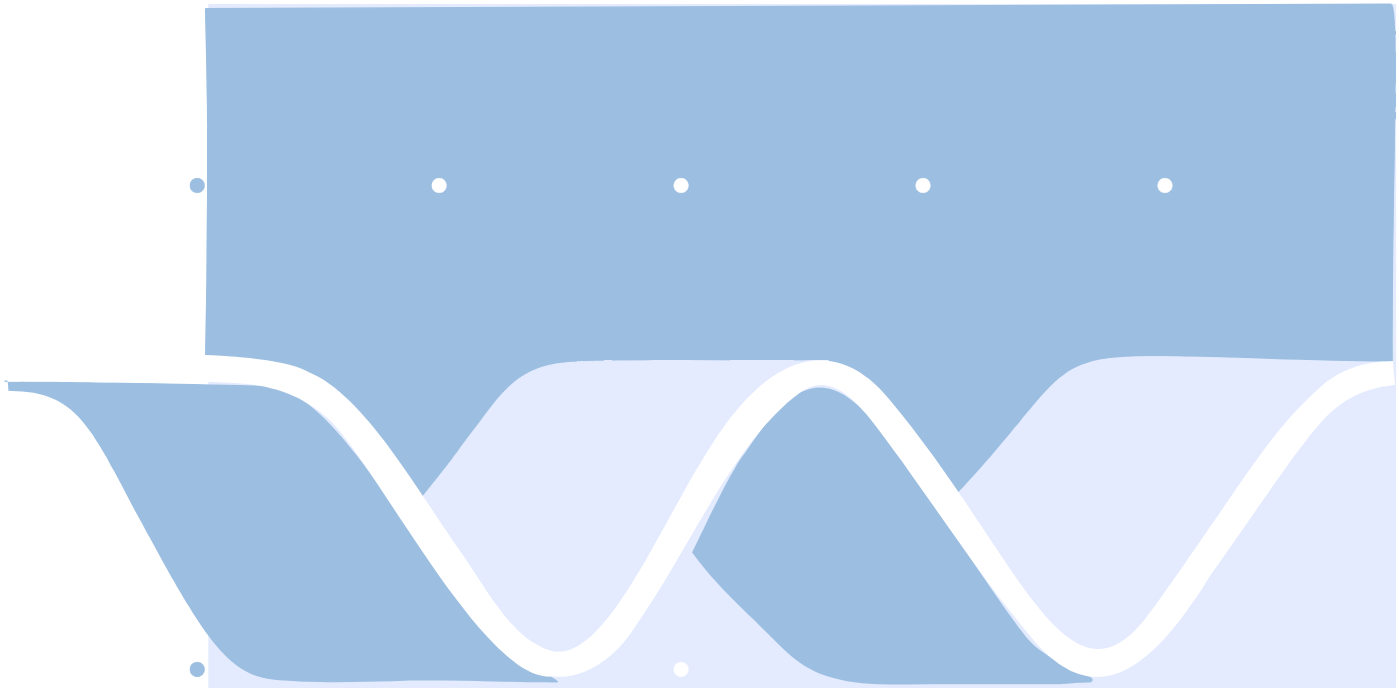

Prepared for:

Commission of the European Communities, CLASH

DG Rijkswaterstaat, RIKZ

Influence of low-frequency waves on wave overtopping

A study based on field measurements at the Petten Sea-defence

M.R.A. van Gent and C.C. Giarrusso

November 2003

H4297

WL | delft hydraulics

WL | delft hydraulics

CLIENTS: Commission of the European Communities, CLASH (EVK-2001-00064)
DG Rijkswaterstaat, RIKZ

TITLE: Influence of low-frequency waves on wave overtopping;
A study based on field measurements at the Petten Sea-defence

ABSTRACT: Within the framework of the European project CLASH phenomena related to wave overtopping are studied. One of the topics that require further attention is the influence of low-frequency waves on wave overtopping. Here, use is made of field measurements performed at the Petten Sea-defence (by Rijkswaterstaat and made available by RIKZ) and numerical models.

During the field measurements storm conditions have been measured. In the present study a series of conditions within the storm period of October 25-28, 2002, have been selected.

Field measurements were analysed to obtain incident waves from the measured surface elevations. This analysis shows that the dike reflects low-frequency waves up to 100% (on average 61%), while wave reflection coefficients based on the energy in the short waves are on average 23%.

Two numerical models have been applied, one for wave propagation over the foreshore and one for the wave motion on the dike. The model for wave propagation over the foreshore TRITON has been used to study whether the amount of low-frequency energy can be computed accurately and it has been applied to obtain wave conditions at the toe of the dike.

Time-signals from measurements and computations have been used as input for the numerical model ODIFLOCS that can simulate wave overtopping. Because the Petten Sea-defence is so high that no wave overtopping occurs, in the computations a crest lower than the actual crest has been applied. The results of this analysis indicate that for the studied storm conditions low-frequency energy increases the mean overtopping discharge with a factor up to a maximum of 5. This increase depends on the percentage of low-frequency energy. For the analysed storm period 'October 2002', a much lower factor was found (up to 1.4). Also for a condition considered as a 'super storm condition' a factor of 1.4 was found. A factor of 1.4 would have a rather small effect on the required crest elevation due to the influence of low-frequency energy.

REV.	ORIGINATORS		DATE	REMARKS	REVIEW		APPROVED BY	
0	M.R.A. van Gent		Nov. 2003		A. van Dongeren		W.M.K. Tilmans	
	C.C. Giarrusso							

KEYWORDS	STATUS
Field measurements Numerical modelling Wave overtopping Dikes Low-frequency waves	☐ PRELIMINARY ☐ DRAFT ☒ FINAL

PROJECT IDENTIFICATION: H4297

Contents

List of Tables

In text:

In Appendix Tables:

List of Figures

In text:

In Appendix Figures:

List of Symbols

Roman letters:

E	:	energy density (m^2/Hz)
f	:	friction coefficient (-)
f_{LFE}	:	factor of increase of mean wave overtopping discharge due to LFE (-)
f_p	:	scaling parameter for wave breaking in Boussinesq-type model (-)
g	:	gravitational acceleration (m/s^2)
$H_{1/3}$	:	significant wave height; mean of the highest one-third of the waves (m)
H_{m0}	:	spectral 'significant wave height', $H_{m0} = 4\sqrt{m_0}$ (m)
H_s	:	significant wave height; mean of the highest one-third of the waves: $H_{1/3}$ (m)
h	:	water depth (m)
K_R	:	reflection coefficient (-)
k	:	wave number (-)
m_n	:	n^{th} moment of the frequency spectrum.
m_0	:	variance of the water surface elevation, *i.e.* the total wave energy (m^2)
q	:	mean overtopping discharge (l/s/m)
$T_{m-1,0}$	:	wave period based on zero and first negative spectral moment (s)
$t_{1/2}$	:	measure related to the time required for the wave to pass through the breaking process (s)
u	:	velocity (m/s)

Greek letters:

δ	:	roller thickness in Boussinesq-type model (m)
φ	:	slope of structure (°)
ν_t	:	turbulence viscosity (m^2/s)
ϕ_{ini}	:	angle of the surface for initiation of wave breaking (°)
ϕ_{ter}	:	angle of the surface for which wave breaking is terminated (°)

Abbreviations:

LFE	:	Low-frequency energy.
NAP	:	Dutch vertical reference level.
SWL	:	Still Water Level, relative to NAP (m)
TE	:	Total energy.

1 Introduction

1.1 General

The crest elevation of dikes is determined on the basis of estimates of wave overtopping discharges. For instance, dikes along parts of the Dutch coast have a crest elevation such that a maximum mean overtopping discharge of 1 l/s/m can occur. These estimates of wave overtopping discharges are based on empirical formulae that require the wave conditions at the toe of the dike. The wave conditions at the toe of the dike are different from those at deep water. Numerical models are used to compute the wave propagation over the foreshore to provide the wave conditions at the toe of the dike. Especially for shallow foreshores this wave propagation is complex, for instance due to the effects of wave breaking. Wave breaking on shallow foreshores involves not only dissipation of energy but also a transfer of wave energy to other wave frequencies, for instance from short waves to low-frequency waves (*i.e.*, 'long waves'). Nowadays, procedures to assess the wave conditions at the toe of dikes do not take into account energy in low-frequency waves. This means that part of the wave energy is neglected. Therefore, it is relevant to study the possible influence of low-frequency waves on wave overtopping.

1.2 Purpose of the study

The purpose of the study described in this report is to provide insight into the possible influence of low-frequency waves on mean wave overtopping discharges. For this purpose, field measurements on the foreshore of the Petten Sea-defence and numerical model results are used.

1.3 Outline

A few aspects related to the occurrence of low-frequency waves in the field measurements on the foreshore of the Petten Sea-defence are analysed in Chapter 2 (*i.e.*, 'percentage of energy present in low-frequency waves' and 'the amount of wave reflection in relation to wave frequencies'). The field measurements provide wave conditions at several positions on the foreshore but they do not provide the wave conditions at the toe. In Chapter 3 the numerical modelling of wave propagation over the shallow foreshore of the Petten Sea-defence is described. This model is used to provide wave conditions, including low-frequency waves, at the toe of the dike. Since wave overtopping did not occur in the field measurements, and is very unlikely to occur at the Petten Sea-defence in general, a

numerical model is used to analyse the possible influence of low-frequency waves on wave overtopping. This is described in Chapter 4. For this analysis with the numerical model computations, a crest elevation lower than the actual crest is applied such that wave overtopping occurs. Finally, Chapter 5 provides an overview of the main conclusions with suggestions for further investigations on the influence of low-frequency waves on wave overtopping.

2 Field measurements

2.1 Introduction

Rijkswaterstaat performed field measurements at the Petten Sea-defence. This site concerns a dike with a shallow foreshore. Waves have been measured at several locations on the foreshore, and also wave run-up measurements have been performed during a number of storm events. A description of the field measurements is given in De Kruif (2000) and Hordijk (2003). All data-signals from these field measurements have been provided by Rijkswaterstaat-RIKZ.

Storms measured in January 1995 have been used for analysis in a number of studies. This concerns for instance an analysis of low-frequency waves (*e.g.* De Haas *et al*, 1999), comparisons with physical model tests (Van Gent, 1999, 2001; Van Gent, De Kruif and Murphy, 2001), and comparisons with numerical models (Van Gent and Doorn, 2001).

The present study is mainly focussed on the storm period October 25-28, 2002. During this storm more measurement equipment was operational than during previous storms. Important is to note that the sandy foreshore has not been stable over the years; fluctuations have been observed from year to year, from season to season, and also within storms.

The Petten Sea-defence is high, so high that the probability of occurrence of wave overtopping events is very small. Therefore, the present study focuses on the measured wave conditions in combination with a numerical model that can simulate wave overtopping for observed wave conditions.

2.2 Description of field measurements

The structure studied here concerns the Petten Sea-defence in The Netherlands. This is an impermeable dike with a berm. The foreshore contains several shallow regions, *i.e.* sand bars on which wave breaking occurs during storms. The depth-contours at this site are close to parallel to the coast and the angle of wave attack during storm conditions is mainly perpendicular. Therefore, a 1D approach has been followed in this study.

A description of the field site and the measurement equipment is given in De Kruif (2000). A picture of the Petten Sea-defence is given in Figure 2.1. The groins shown in this picture have a length of 70 m and a separation of 120 m. Wave run-up is measured in the middle of 2 of these groins. Figure 2.2 shows a picture of wave run-up on the Petten Sea-defence during a storm.

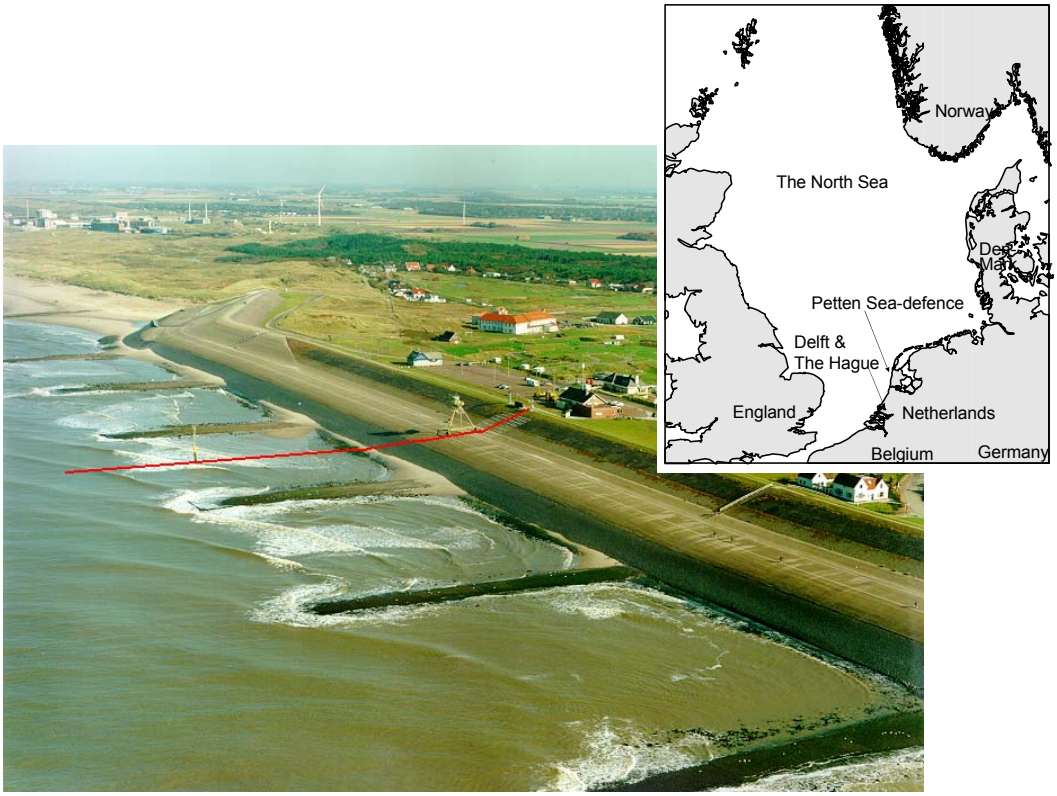

Figure 2.1 Aerial photograph of the Petten Sea-defence with the cross-section in which measurements are performed indicated (groins have a length of 70 m and a separation of 120 m).

Figure 2.2 Photograph of a wave run-up event on the Petten Sea-defence during a storm (on the left the berm is covered with water; on the right wave run-up is at its maximum at the measurement section, with piles close to the step-gauge).

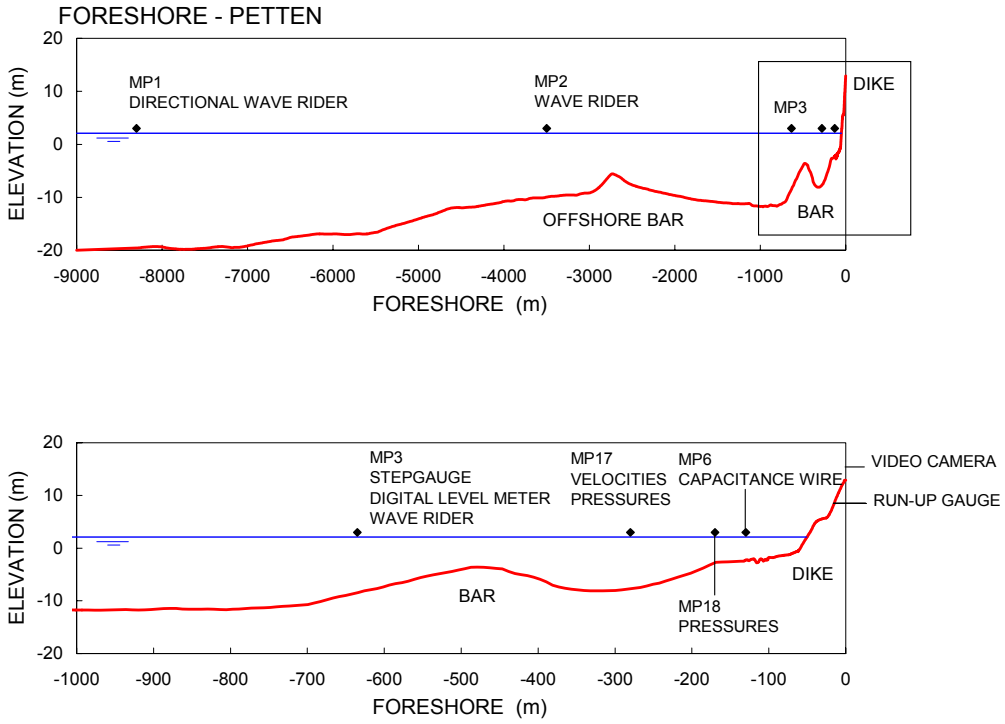

Figure 2.3 Cross-section of the foreshore with the locations of equipment.

Graphs in Figure 2.3 show the foreshore perpendicular to the dike (after storms in 1995). Between 7 and 3 km offshore, the depth gradually decreases from -20 m to -10 m, (these levels are relative to the Dutch vertical reference level NAP), with an average slope of approximately 1:400. Then the foreshore contains an offshore bar with a crest at approximately -6 m, on which wave breaking occurs during storms. Landward of the offshore bar the depth increases again to -12 m at about 1 km from the dike. The lower graph in Figure 2.3 shows the foreshore in the last kilometre and the position of the most essential equipment. This last kilometre was also modelled in a study based on physical model tests. A second bar with a crest at about -3.5 m is present at about 500 m seaward from the crest of the dike, where again wave breaking occurs during storms. The foreshore just in front of the toe of the dike is also in shallow water. Here, for the third time a breaker zone is present during storm conditions.

At 8300 m (MP1) and 3500 m (MP2) from the crest of the dike wave riders were located, of which MP1 is a directional wave rider. At about 610 m (MP3) and 125 m (MP6) poles are positioned with a step-gauge (MP3) and a pressure transducer (MP6). At a few locations equipment has been installed which was not present during for instance storms that occurred in January 1995. At about 280 m (MP17) velocities have been measured and also pressures to obtain surface elevations. This allows for incident and reflected waves to be separated. At about 170 m (MP18) also pressures have been measured to obtain surface elevations.

The dike consists of a 1:4.5 lower slope, a berm of about 1:20 and a 1:3 upper slope. The crest elevation is NAP+12.9 m. Wave run-up levels were measured at the upper slope by sensors, acting as a step-gauge, within the smooth slope.

2.3 Analysis of low-frequency energy

The storm period of October 25 to 28, 2002 has been analysed on the occurrence of low-frequency waves. To simplify this analysis, periods of about 2 hours have been selected. Most of them have been selected because the mean water level did not vary significantly. Figure 2.4 shows the variation of the mean water level at MP3 in above mentioned storm period, and the 17 selected periods of 2 hours.

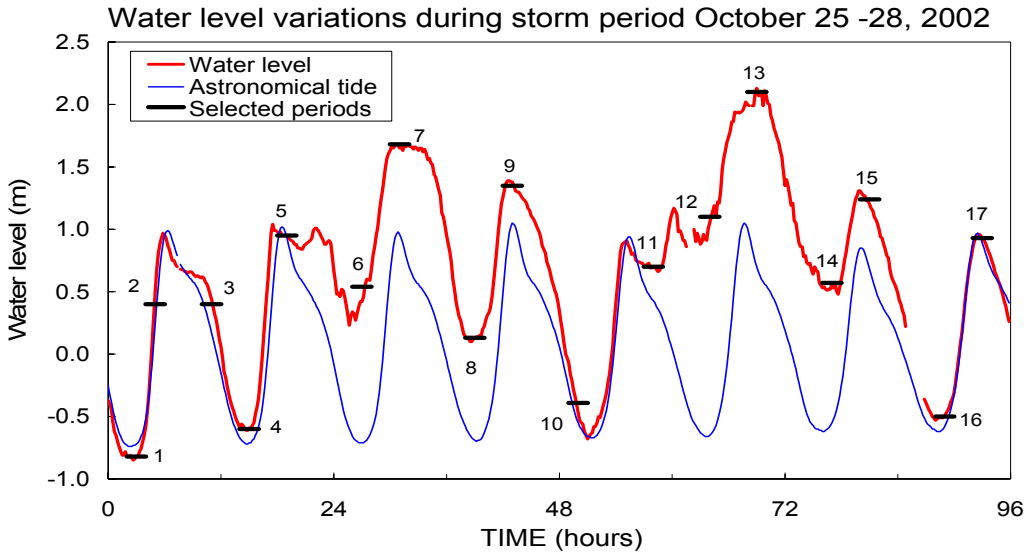

Figure 2.4 Water level variations during storm period (at MP3).

Periods with a rather constant mean water level occur during low and high water. In total 17 periods have been selected in which most of the essential equipment functioned properly. For these 17 selected periods measured wave heights and wave periods are obtained at 4 locations (*i.e.*, MP3, MP17, MP18 and MP6). Figure 2.3 shows the position of these locations. Figure 2.5 shows the significant waves heights at MP3 and MP6 in these periods.

In this study low-frequency energy is considered as the energy in frequencies lower than 0.04 Hz. In the Appendix 'Tables' for each location (*i.e.*, MP3, MP17, MP18 and MP6) the percentage of energy in low-frequencies is given (Tables T1.1-T1.4), the wave height H_{m0} obtained from the short waves (0.04 Hz $< f <$ 0.5 Hz), from the low-frequency waves (0.01 Hz $< f <$ 0.04 Hz), and the total wave field including low-frequency energy for wave periods larger than 100 s (0.01 Hz $< f <$ 0.5 Hz). Also the wave period $T_{m-1,0}$ is given. Table 2.1 shows this overview for the location MP6.

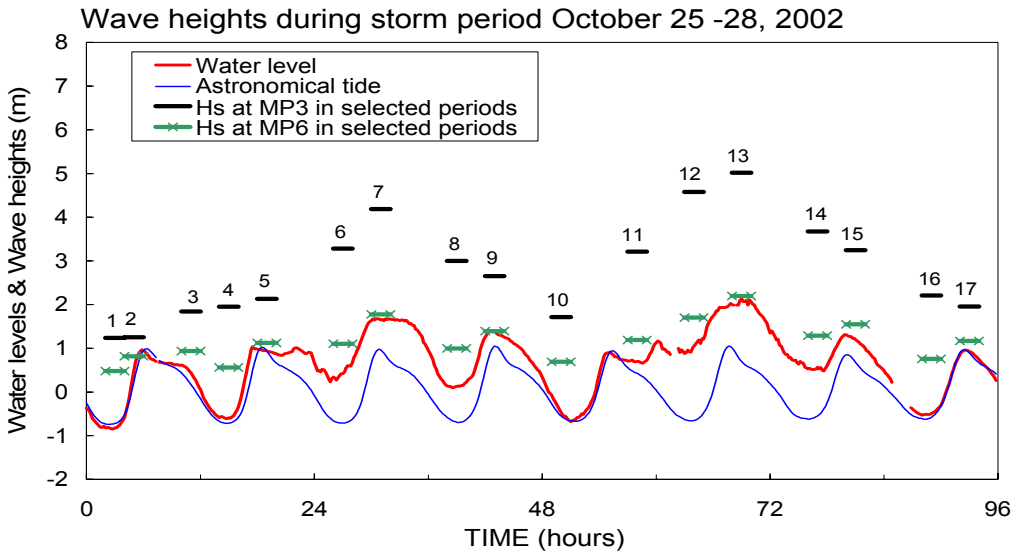

Figure 2.5 Wave heights at MP3 and MP6 during selected periods.

From these results it can be concluded that for the analysed signals from storm conditions within the period of October 25 to 28, the amount of energy in low-frequencies is low. As expected the amount of energy in low-frequencies increases in the direction of the dike. At MP6 the percentage of energy in low-frequencies compared to the total energy is in the range of 2% to 8%.

MP6								
No	*Date*	*Time (hour)*	*MWL (NAP)*	*LFE / TE (-)*	H_{m0} *(short)*	H_{m0} *(LFE)*	H_{m0} *(total)*	$T_{m-1,0}$ *(total)*
1	25-10-2002	2-4	-0.74	0.05	0.48	0.11	0.50	11.4
2	25-10-2002	4-6	0.37	0.02	0.82	0.10	0.83	10.6
3	25-10-2002	10-12	0.37	0.02	0.93	0.14	0.94	8.0
4	25-10-2002	14-16	-0.52	0.06	0.55	0.14	0.56	10.8
5	25-10-2002	18-20	0.93	0.03	1.14	0.19	1.16	8.8
6	26-10-2002	2-4	0.56	0.08	1.11	0.32	1.15	11.5
7	26-10-2002	6-8	1.77	0.05	1.74	0.39	1.78	10.9
8	26-10-2002	14-16	0.23	0.07	0.99	0.27	1.02	11.6
9	26-10-2002	18-20	1.34	0.03	1.37	0.25	1.40	9.3
10	27-10-2002	1-3	-0.37	0.05	0.69/NR	0.15/NR	0.70/NR	10.4/NR
11	27-10-2002	9-11	0.77	0.05	1.20	0.27	1.23	10.6
12	27-10-2002	15-17	1.32	0.07	1.67	0.48	1.74	13.5
13	27-10-2002	20-22	2.21	0.06	1.87	0.47	1.93	12.5
14	28-10-2002	4-6	0.68	0.07	1.29	0.36	1.34	12.4
15	28-10-2002	8-10	1.20	0.04	1.50	0.32	1.54	10.8
16	28-10-2002	16-18	-0.37	0.06	0.76	0.19	0.78	11.2
17	28-10-2002	20-22	0.89	0.02	1.19	0.18	1.20	8.9

These wave conditions are based on analysis of signals of surface elevations including reflected waves.
NAP: Dutch vertical reference level.
LFE: Low-frequency energy (0.01 Hz – 0.04 Hz)
TE: Total wave energy (0.01 Hz – 0.5 Hz)
NR: Not Reliable

Table 2.1 Measured storm conditions at MP6.

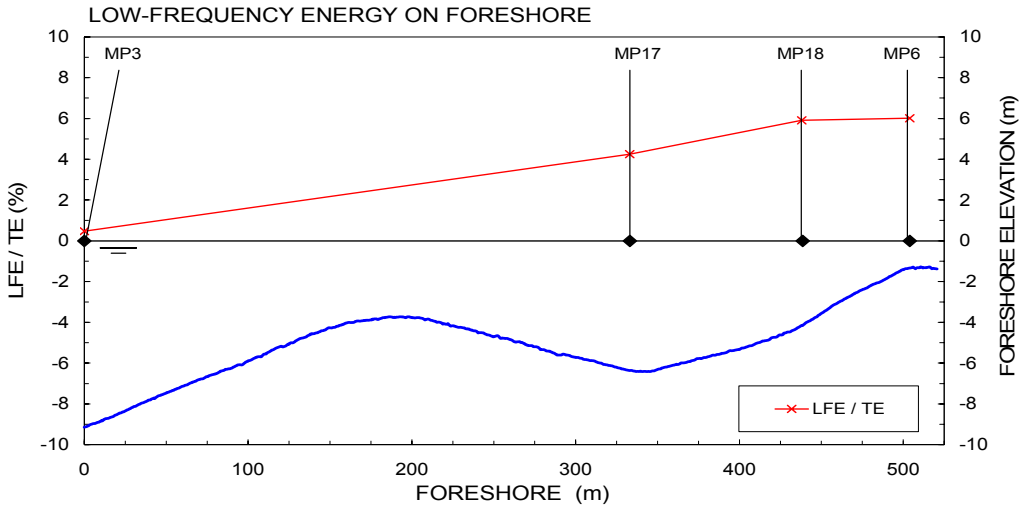

Figure 2.6 Measured percentage of low-frequency energy at several positions on the foreshore (condition 13).

Figure 2.6 shows an example of the ratio of low-frequency energy (LFE) and the total energy (TE) as measured at MP3, MP17, MP18 and MP6. This figure shows that there is a clear increase of this ratio between MP3 and MP6. In the Appendix 'Figures' this type of graph is shown for each of the selected periods (Figures F1.x).

2.4 Analysis of wave reflection

Structures such as the Petten Sea-defence cause wave reflection. Therefore, measurements of surface elevations contain both incident waves and reflected waves. These cannot be separated in measurements of surface elevations at a single position. Nevertheless, the incident waves are required as boundary conditions to assess wave run-up levels and wave overtopping discharges. Therefore, Rijkswaterstaat installed equipment to measure velocities at the position MP17. This allows for analysis of wave reflection.

For the conditions listed in Table 2.2 wave reflection characteristics have been analysed. This table provides two types of reflection coefficients for each condition, one based on the ratio of reflected and incident *wave heights* and one based on the ratio of reflected and incident *energy*. The total wave reflection coefficients are based on energy between 0.01 Hz and 0.2 Hz. It should be noted that the accuracy of the method to separate incident and reflected waves from measured surface elevations becomes less for shorter waves (frequencies higher than 0.2 Hz). Although at wave frequencies higher than 0.2 Hz there is still a considerable amount of wave energy, this energy has not been taken into account in the obtained reflection coefficients. Also reflection coefficients based on energy in low frequencies (0.01 Hz – 0.04 Hz), and in short waves (0.04 Hz – 0.2 Hz) have been obtained.

MP17								
No	*Date*	*Time*	K_R *(wave heights)*			K_R *(energy)*		
		(hour)	$K_{R\text{-}TOTAL}$	$K_{R\text{-}LFE}$	$K_{R\text{-}SHORT}$	$K_{R\text{-}TOTAL}$	$K_{R\text{-}LFE}$	$K_{R\text{-}SHORT}$
1	25-10-2002	2-4	0.37	0.64	0.36	0.13	0.41	0.13
2	25-10-2002	4-6	0.47	0.81	0.46	0.22	0.65	0.22
3	25-10-2002	10-12	0.51	0.64	0.51	0.26	0.41	0.26
4	25-10-2002	14-16	0.48	0.67	0.48	0.24	0.44	0.23
5	25-10-2002	18-20	0.48	0.67	0.48	0.23	0.44	0.23
6	26-10-2002	2-4	0.57	0.87	0.56	0.33	0.76	0.32
7	26-10-2002	6-8	0.57	0.95	0.56	0.33	0.90	0.31
8	26-10-2002	14-16	0.45	0.80	0.44	0.20	0.64	0.19
9	26-10-2002	18-20	0.42	0.73	0.41	0.17	0.53	0.17
10	27-10-2002	1-3	0.37	0.58	0.37	0.14	0.33	0.13
11	27-10-2002	9-11	0.60	0.99	0.58	0.36	0.99	0.34
12	27-10-2002	15-17	0.67	0.94	0.66	0.46	0.88	0.43
13	27-10-2002	20-22	0.58	0.88	0.57	0.34	0.77	0.33
14	28-10-2002	4-6	0.42	0.73	0.41	0.18	0.53	0.17
15	28-10-2002	8-10	0.39	0.84	0.38	0.15	0.70	0.14
16	28-10-2002	16-18	0.38	0.56	0.38	0.15	0.31	0.15
17	28-10-2002	20-22	0.40	0.84	0.39	0.16	0.71	0.16
AVERAGE			0.48	0.77	0.47	0.24	0.61	0.23

$K_{R\text{-}TOTAL}$: reflection coefficient based on energy between 0.01 Hz and 0.2 Hz.
$K_{R\text{-}LFE}$: reflection coefficient based on energy between 0.01 Hz and 0.04 Hz.
$K_{R\text{-}SHORT}$: reflection coefficient based on energy between 0.04 Hz and 0.2 Hz.

Table 2.2 Wave reflection coefficients at MP17.

Wave reflection is not the same for each wave frequency; longer waves are normally reflected more than shorter waves. To illustrate this, figures are given in the Appendix 'Figures' for each of the 17 selected conditions (Figures F2.x). Figure 2.7 shows an example that illustrates that wave reflection for low-frequency waves $K_{R\text{-}LFE}$ is much higher (on average 61%, based on energy) than the wave reflection for short waves $K_{R\text{-}SHORT}$ (on average 23%, based on energy). For higher wave frequencies the method becomes less accurate (right side of these figures).

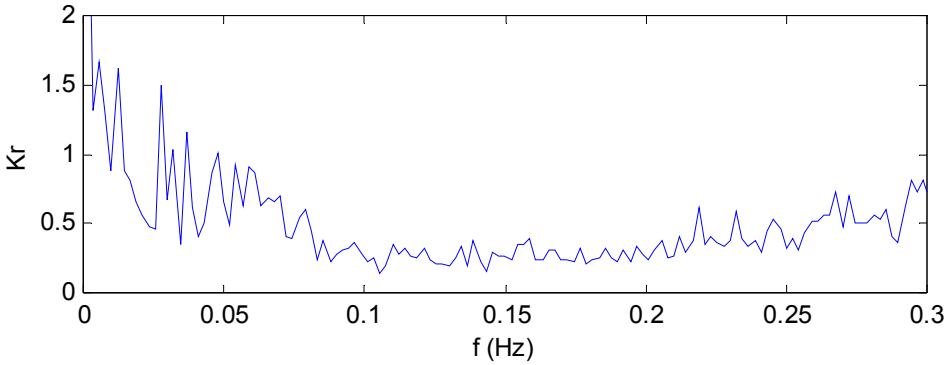

Figure 2.7 Wave reflection as function of wave frequency (condition 13); measured at MP17.

2.5 Discussion of results

The analysis of specific aspects of the field measurements resulted in the following findings:

- Measured wave reflection is on average 61% for low-frequency energy, but for some frequencies it can be considerably higher than 100% due to the generation of low-frequency waves in the region landward of MP17.
- The wave reflection coefficients based on the ratio of the reflected and incident wave energy resulted in an average of 24% for the conditions within the storm period of October 25 to 28, 2002.
- Analysing the evolution of low-frequency waves over the foreshore showed that the contribution of low-frequency energy to the total wave energy increases between MP3 (at about 610 m from the dike) and MP6 (at about 125 m from the dike).
- At MP6 the measured amount of low-frequency energy was on average 5% of the total energy, with a maximum of 8%; 5% in energy means that the H_{m0} based on the energy in the low frequencies is 22% of the wave height based on all energy.

Although the measured amount of low-frequency energy is rather low, these measurements will be used for further analysis of the possible influence of this wave energy on mean wave overtopping discharges.

3 Modelling of wave propagation

3.1 Introduction

Low-frequency waves play an important role in situations with wave breaking because during wave breaking low-frequency waves are generated. Since wave breaking occurs in the shallow parts of the foreshore, while the toe is often in the shallowest part, the amount of low-frequency energy at the toe can be quite large. It is not appropriate to use conditions seaward of the toe for wave overtopping estimates because in the region close to the dike important changes are likely to occur with respect to low-frequency waves.

To analyse low-frequency waves a numerical model capable of modelling the transfer of energy from short waves to low-frequency waves is used. This allows for studying low-frequency waves in the region close to the dike, and other (more severe) conditions than those that have been measured.

In this chapter first the numerical model is briefly described, then computations that have been performed. Finally, an analysis of low-frequency waves at the toe of the dike is given.

3.2 Description of numerical model

The numerical model applied in the part of the study described in this chapter is a time-domain model which can simulate wave propagation over foreshores. The model that has been applied is the Boussinesq-type model TRITON developed at Delft Hydraulics. This model is described briefly in this section. A more detailed description can be found in Borsboom *et al.* (2000, 2001-a,b) and Groeneweg *et al.* (2002).

Boussinesq-type wave models are in principle suitable to model wave propagation in coastal regions and harbours. Especially for the wave propagation of short waves, where non-linear effects, dispersion and shoaling play an important role, this type of model can be adequately applied and provide valuable information on the wave field (*e.g.*, time series of surface elevations and velocities in shallow regions) which cannot accurately be obtained from many other types of models.

Within the range of existing Boussinesq-type models, each model aims for a certain accuracy of *a)* non-linear effects, *b)* linear dispersion and *c)* shoaling. The accuracy of each of these three aspects should be in balance: Improving linear dispersion without sufficiently improving the non-linear effects might be inadequate if wave propagation over shallow foreshores is concerned. On the other hand, improving each of the aspects where the three

aspects are in balance, might lead to a very complex model which may result in large computing times. The Boussinesq-type model applied here is a model developed to obtain an accuracy as good as possible within limited computing times. Besides a proper balance between accuracy and computing time also a proper balance was found between the accuracy of the mathematical description and the accuracy of the numerical schematisation. In addition, the applied model has a few unique properties for a Boussinesq-type model:

- The formulation is independent of the vertical reference level for bottom topography and water elevation, which facilitates straightforward practical applications.
- Dispersion and shoaling are modelled in a very compact way, which reduces computing times.
- Both mass and momentum are conserved, which means that the model, besides providing solutions of the applied formulations, also assures that basic physical properties are modelled correctly.

The equations of the 2D Boussinesq-type model, which is applied in a 1D situation here, can be written as follows:

$$\frac{\partial h}{\partial t} + \nabla \cdot \mathbf{q} = 0 \tag{3.1}$$

$$\frac{\partial \mathbf{u}}{\partial t} + \left[\nabla\left(\bar{\mathbf{u}}\mathbf{q}\right)\right]^{\mathrm{T}} + \nabla P = p_b \nabla h_R \tag{3.2}$$

$$\text{with} \qquad P = g\frac{\tilde{h}^2}{2}, \qquad p_b = g\left(\frac{3\tilde{h}}{2} - \frac{h}{2} + \frac{h}{4}\nabla h \cdot \nabla \zeta\right) \tag{3.3}$$

$$\text{and} \qquad \tilde{h} - \alpha h^2 \nabla^2 \tilde{h} - \beta h \nabla h_R \cdot \nabla \tilde{h} =$$
$$= h + \left(\frac{1}{3} - \alpha\right) h^2 \nabla^2 h + \left(\frac{1}{2} - \beta\right) h \nabla h_R \cdot \nabla h - \frac{1}{3} h^2 \nabla^2 h_R - \frac{1}{2} h \nabla h_R \cdot \nabla h_R \tag{3.4}$$

The unknowns in these equations are the total water depth h and the depth-integrated velocity vector $\mathbf{q}$; the bathymetry is described with respect to some arbitrary reference level h_R. From these variables the water elevation with respect to the reference level $\zeta = h - h_R$ and the depth-averaged velocity vector $\bar{\mathbf{u}} = \mathbf{q}/h$ are obtained. Auxiliary variable $\tilde{h}$ is a function of h, defined implicitly by Equation 3.4. This equation realises a so-called [2,2] Padé approximation of linear dispersion and the first order effect of linear shoaling that can be adjusted by respectively α and β. The value of these parameters should be 0.4 or slightly lower. Auxiliary variables P and p_b have been introduced because of their physical meaning. From the conservative form of momentum equation (3.2) it can be seen that P and p_b must represent respectively the depth-integrated pressure and the pressure at the bottom, both divided by the density that is assumed constant.

Wave breaking is implemented based on a new method by Borsboom *et al* (2001-a) where wave breaking is modelled as an eddy-viscosity model in combination with a surface roller.

Wave breaking is implemented as an eddy-viscosity model as for instance also applied by Kennedy *et al.* (2000):

$$\frac{\partial}{\partial x_w} h \nu_t \frac{\partial \overline{u}_w}{\partial x_w} \tag{3.5}$$

where x_w is the propagation direction of the wave, h is the water depth, $\overline{u}_w$ is the depth-averaged flow velocity in x_w-direction and ν_t is the turbulence-viscosity coefficient, which is averaged over the depth. For the determination of ν_t use is made of the concept of surface rollers (Schäffer *et al.*, 1992). The idea behind this concept is as follows: Wave breaking is assumed to initiate if the slope of the local water surface exceeds a certain value ϕ_{ini} and assumed to finish if the slope of the local water surface becomes below a certain value ϕ_{ter}. The water above the tangent of this critical slope is assumed to belong to the roller. This slope is assumed to vary in time while being constant in space within each surface roller:

$$\tan\phi = \tan\phi_{ini} + (\tan\phi_{ter} - \tan\phi_{ini}) \exp\left[-\ln 2 \frac{t - t_b}{t_{1/2}} \right] \tag{3.6}$$

The turbulence-viscosity coefficient that is used in the present model is scaled with the height of this surface roller:

$$\nu_t = f_p \delta (c - \overline{u}) \tag{3.7}$$

where δ is the roller height, c is the local wave celerity modelled as $c = 1.3\sqrt{gh}$ and f_p is the parameter that is used for scaling. The model makes use of four coefficients of which the values are based on a sensitivity-analysis using a selection of tests from the present data-set. These coefficients are kept constant in all computations. The initial angle of the surface for which breaking starts ϕ_{ini} is estimated to be in the order of 15° which exponentially changes to the terminal breaking angle ϕ_{ter} which is in the order of 10°. The parameter $t_{1/2}$ is a measure related to the time required for the wave to pass through the breaking process. The following value $t_{1/2} = T_m/10$ is used. The amount of energy dissipation can be scaled with the parameter f_p for which a value of 30 has been used.

Another important aspect of the model is the modelling of weakly reflecting boundaries, based on the concepts by Borsboom *et al.* (2000, 2001-b). A validation of the model based on measured conditions on the foreshore of Petten is given in Van Gent and Doorn (2001).

3.3 Description of numerical model computations

In the present analysis two series of computations have been used:

- Storm conditions ‘January 1995’
- Storm conditions ‘October 2002’

The first set of computations was already performed and presented in Van Gent and Doorn (2001) but the validation was focussed on short waves only. It concerned 6 storm conditions from field measurements in 1995, which were reproduced in an earlier study based on physical model tests. Another series of 14 storm conditions were tested and also computed with the described numerical model. One of these conditions (*i.e.*, 2.54) is denoted here by 'super storm condition'. In the analysis of the computational results, no analysis was made on the amount of low-frequency energy. Therefore, these computations have been reanalysed with respect to the amount of low-frequency energy, see the following section.

The second set of computations concerns a number of selected storm conditions from the storm period October 2002. Because the breaker module of the model TRITON is under further development, without reaching the final result yet, the version applied here is neither the same as the one used in above mentioned computations performed a few years ago, nor the improved and calibrated breaker module which is under development. The results presented here are therefore not really representative for the numerical model, and will be outdated within the coming months.

3.4 Low-frequency energy

Storm conditions 'January 1995'

For 20 conditions numerical model computations were performed for validation of low-frequency waves during conditions that were tested in a study based on physical model tests (Van Gent and Doorn, 2001). For these conditions the ratio of the energy in low-frequency waves (LFE) compared to the total wave energy has been analysed, both for the measurements and for the performed computations. Here, low-frequency energy is defined as energy between the frequencies 0.01 Hz and 0.04 Hz, and the total wave energy between the frequencies 0.01 Hz and 0.05 Hz. Table 3.1 shows for each condition the results.

Table 3.1 gives (for each condition):

- the ratio of computed and measured total energy; on average the computations overestimate the total wave energy at the toe with 11%.
- the ratio of low-frequency energy and the total wave energy for the *measured* time-signals; on average 22% of the total energy is in low-frequency waves.
- the ratio of low-frequency energy and the total wave energy for the *computed* time-signals; on average 20% of the total energy is in low-frequency waves.
- the differences (in %) between the computed and measured ratios; on average the computations underestimate the percentage of low-frequency energy with 1.4%, with maximum differences of an overestimate of about 10% and an underestimate of about 10%.

Validation of LFE computed by TRITON					
No.	*SWL*	*TE*	*LFE / TE*	*LFE / TE*	*DIFFERENCE*
	(NAP)	*COMP/MEAS*	*MEASURED*	*COMPUTED*	*%*
1.01	2.10	1.13	0.25	0.23	-2.3
1.02	2.04	1.12	0.30	0.24	-5.9
1.03	2.24	1.15	0.29	0.22	-6.8
1.04	1.66	1.01	0.45	0.38	-7.6
1.05	1.60	1.12	0.27	0.26	-0.4
1.06	2.04	1.02	0.25	0.19	-5.8
2.11	2.10	1.35	0.11	0.06	-4.4
2.13	2.10	1.12	0.22	0.27	4.9
2.15	2.10	1.25	0.35	0.36	1.8
2.21	4.70	1.50	0.02	0.01	-0.6
2.23	4.70	1.12	0.07	0.09	1.8
2.25	4.70	1.13	0.11	0.16	4.5
2.31	2.10	0.96	0.15	0.15	-0.2
2.41	4.70	0.95	0.03	0.03	0.4
2.51	4.70	0.95	0.09	0.11	1.6
2.54	4.70	1.25	0.10	0.20	9.3
2.61	1.30	1.18	0.30	0.30	-0.5
2.71	2.10	0.98	0.27	0.21	-5.2
2.72	2.10	0.94	0.38	0.28	-10.2
2.73	2.10	0.99	0.33	0.31	-1.9
AVERAGE		1.11	0.22	0.20	-1.4
LFE: Low-frequency energy (0.01 Hz < f < 0.04 Hz) TE: Total energy (0.01 Hz < f < 0.5 Hz) For more information on the wave conditions see Van Gent (1999).					

Table 3.1 Measured and computed wave energy in low-frequency waves at the toe ('January 1995').

From this analysis it can be concluded that the model is capable of providing good estimates of the amount of low-frequency waves for these 20 storm conditions. Figure 3.1 illustrates the accuracy of the numerical model.

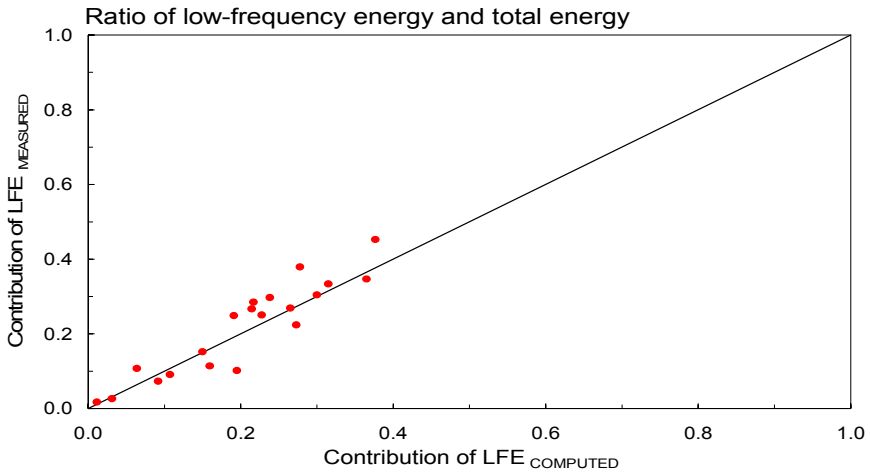

Figure 3.1 Comparison between measured and computed contribution of low-frequency energy.

Storm conditions 'October 2002'

In Chapter 2 17 periods of 2 hours within the storm period of October 25-28, 2002 have been analysed. For a selection of these conditions numerical model computations have been performed. In the Appendix 'Figures' measured and computed wave energy spectra are shown for all computed conditions (Figures F3.x). From these figures it can be observed that for most conditions the computed amount of energy at MP17, MP18 and MP6 is higher than measured. This is also valid for the amount of low-frequency energy.

Validation of LFE computed by TRITON					
No.	*SWL*	*TE*	*LFE / TE*	*LFE / TE*	*DIFFERENCE*
	(NAP)	*COMP/MEAS*	*MEASURED*	*COMPUTED*	*%*
1	-0.74	6.5	0.05	0.03	-2.1
5	0.93	3.1	0.03	0.03	0.0
7	1.77	3.8	0.05	0.05	0.5
8	0.23	4.7	0.07	0.06	-0.8
9	1.34	3.3	0.03	0.04	0.5
10	-0.37	5.0	0.05	0.05	0.0
11	0.77	5.3	0.05	0.05	0.5
13	2.21	5.8	0.06	0.04	-1.6
17	0.89	2.4	0.02	0.04	1.5
AVERAGE		4.4	0.04	0.04	-0.2
LFE: Low-frequency energy (0.01 Hz < f < 0.04 Hz) TE: Total energy (0.01 Hz < f < 0.5 Hz) NR: Not Reliable					

Table 3.2 Measured and computed wave energy in low-frequency waves at MP6 ('October 2002').

Table 3.2 shows (for each condition):

- the ratio of computed and measured total energy; on average the computations overestimate the total wave energy at MP17 with a factor 2.8, at MP18 with a factor 2.2 and at MP6 with a factor 4.4 (see also Tables T2.1-T2.3 in the Appendix 'Tables').
- the ratio of low-frequency energy and the total wave energy for the *measured* time-signals used for comparison; on average 4% of the total energy is in low-frequency waves, with a maximum of 7%.
- the ratio of low-frequency energy and the total wave energy for the *computed* time-signals; on average 4% of the total energy is in low-frequency waves, with a maximum of 6%.
- the differences (in %) between the computed and measured ratios; on average the differences in the percentage of low-frequency energy are less than 1%, with maximum difference of about 1.6%.

From the analysis of conditions observed in the storm period of 'October 2002' it can be concluded that the model overestimates the total amount of wave energy at the toe. Also the amount of low-frequency energy is higher than obtained from the field measurements. The measured conditions show a relatively low amount of low-frequency energy, much lower

than in the storms that were measured in the wave flume (with conditions from 'January 1995').

It can be concluded that for the 'October 2002' conditions the numerical model provides good estimates of the ratio of low-frequency energy and the total wave energy at MP6, but this is due to an overestimate of the low-frequency and an overestimate of the total energy.

3.5 Discussion of results

The conditions studied here indicate that:

- the numerical model provides good estimates of the amount of low-frequency waves for conditions that have been measured in physical model tests; the ratio of low-frequency energy and the total wave energy was on average 22% and 20% at the toe of the dike in the measurements and the computations respectively. Six of the 20 conditions resemble storm conditions that were measured in field measurements in January 1995.
- the numerical model overestimates the amount of low-frequency waves for conditions that have been measured in the storm period of October 2002; however, the ratio of low-frequency energy and the total wave energy was on average 4% in the measurements and in the computations. Thus the ratio of energy in low-frequency waves and the total amount of energy is rather accurate.

The reason why the numerical model computations lead to a higher amount of low-frequency energy than obtained from the measurements remains unclear. However, the numerical model computations and the conditions measured in physical model tests correspond to long-crested waves, while in field conditions short-crested waves occur. If short-crested waves lead to a lower amount of low-frequency energy than long-crested waves, this would (at least partly) explain the observed differences.

The numerical model provides time series of waves, including low-frequency waves, at the toe of the dike; these are used in Chapter 4 to obtain estimates of wave overtopping discharges for conditions with and without low-frequency energy.

4 Modelling of wave overtopping

4.1 Introduction

Because wave overtopping did not occur in the field measurements, and because wave overtopping is very unlikely to occur at the Petten Sea-defence in general, a numerical model is used to analyse the possible influence of low-frequency waves on wave overtopping. In the computations with the numerical model ODIFLOCS a structure with a crest elevation (lower than the actual crest of the Petten Sea-defence) is taken such that wave overtopping occurs. The wave conditions that are used as input for the wave overtopping computations are realistic for a moderate storm since they are obtained from wave propagation over the foreshore of the Petten Sea-defence. The structure applied in the computations is artificial since a lower crest is required to obtain wave overtopping. Most of the conditions studied here concern wave motion on the slope underneath the berm of the Petten Sea-defence. This is a 1:4.5 slope. Therefore, all computations have been performed on a dike with a 1:4.5 slope while the crest is taken such that realistic wave overtopping discharges occur (*i.e.*, mainly in the range of 0.1 - 10 l/s/m). For each condition two computations have been performed, one with a wave train including low-frequency energy and one with a wave train with the same (short) waves but without low-frequency energy. This provides insight into the possible influence of low-frequency energy on wave overtopping discharges.

4.2 Description of numerical model

The numerical model applied in this chapter is a time-domain model which can simulate the wave motion on the slope of coastal structures. The model (ODIFLOCS) is described in detail in Van Gent (1994, 1995). In this section a short description of basic aspects is given.

The model allows for simulations of normally incident wave attack on various types of structures. Use is made of the non-linear shallow-water wave equations where steep wave fronts are represented by bores. The model is based on concepts by Hibberd and Peregrine (1979) who developed a numerical model with an explicit dissipative finite-difference scheme (Lax-Wendroff) for impermeable slopes without friction. Using this concept, many practical applications have been performed. See for instance Kobayashi *et al.* (1987) for wave reflection and run-up on impermeable rough slopes. In Van Gent (1994, 1995) these concepts are used and extended such that the model allows for simulations of the wave interaction with permeable coastal structures. The model consists of two coupled regions; one for the external wave motion and one for the permeable part. The basic equations of the model for the external wave motion are:

$$\frac{\partial h\,u}{\partial t} + \frac{\partial h\,u^2}{\partial x} = -\,g\,h\,\frac{\partial h}{\partial x} - g\,h\tan\varphi_s - \frac{1}{2}\,f\,u\,|u| + q\,q_x \tag{4.1}$$

$$\frac{\partial h}{\partial t} + \frac{\partial h\,u}{\partial x} = q \tag{4.2}$$

where h is the thickness of the water layer, u is the depth-averaged velocity, φ_s is the angle of the slope, f is the bottom friction coefficient, q is the volume-flux of the flow between the external and internal (permeable) regions and q_x is the horizontal component of the velocity of this flow.

The model is able to deal with either regular or irregular waves which attack various types of structures with arbitrary seaward slopes, smooth or rough, permeable or impermeable, overtopped or not. Since the non-linear shallow-water wave equation overestimates the non-linear effects, because these effects are not counteracted by frequency dispersion, inaccuracies will occur when wave propagation over long distances is concerned. Therefore, for many applications it is advisable to start the wave simulations at the toe of the structure. On the slope itself the distances are relatively small and non-linear effects are more important than frequency dispersion. Many applications show that sufficiently accurate results can be obtained. The model is applied here because earlier computations already showed that the model can be applied successfully (*e.g.*, Van Gent, 2001, and Van Gent and Doorn, 2001).

The model allows for wave generation with arbitrary wave energy spectra. The time-series can be generated using random phases. Also recordings of measured surface elevations can be used as incident wave trains. At the incident wave boundary reflected waves are allowed to leave the computational domain by assuming linear long waves at this boundary. These assumptions are unlikely to be valid at the toe of a structure. The effects of this assumption and other approximations can be studied by validations with analytical solutions and test-results from physical models. In addition to validations described in Van Gent (1994, 1995), additional comparisons with physical model tests were performed in Van Gent and Doorn (2001). In the present computations the consequences of assuming linear long waves at the seaward boundary for waves of all frequencies have not been analysed.

4.3 Description of numerical model computations

In the present analysis three series of computations have been used:

- Storm conditions ‘January 1995’
- Storm conditions ‘October 2002’
- Super storm condition

Storm conditions 'January 1995'

The first set of computations concerns storm conditions from field measurements in 1995, which were reproduced in physical model tests. Another series of 14 storm conditions that were tested are used here for further analysis. Thus in total 20 conditions have been used in this set of computations. One of these conditions (*i.e.*, 2.54) is denoted here by 'super storm condition', used in the third set of computations. For each condition two computations have been performed, one with a wave train including low-frequency energy and one with a wave train with the same (short) waves but without low-frequency energy. Time signals of incident waves measured at the toe of the dike have been used as input for these computations. For each condition a different crest level has been used such that realistic wave overtopping discharges occur (*i.e.*, mainly in the range of 0.1 - 10 l/s/m).

Storm conditions 'October 2002'

The second set of computations concerns a number of selected storm conditions from the field measurements in the storm period October 25-28, 2002. A selection of 17 conditions has been made (see Chapter 2). Two sub-sets of computations have been performed. First time signals, containing incident and reflected waves, measured at the MP6 have been used as input for the wave overtopping computations. Secondly, output at the toe of the dike from the numerical model computations described in the previous chapter has been used as input. Again for each condition two computations have been performed, one with a wave train including low-frequency energy and one with the same wave train but without low-frequency energy.

Because some of the signals at MP6 (used as input for the computations) were considered as too unreliable for these computations, 3 of the 17 conditions have not been included in this set of computations. Observed problems concerned 'spikes' in the measurement signals, too strong water level variations, and problems due to 'no signal or water at MP6' during the trough of waves. A method to deal with 'spikes' has been applied. Nevertheless, these spikes cause inaccuracies in the applied time-signals, also after 'correcting' the signals.

Super storm condition

One of the conditions tested in the model tests mentioned above ('January 1995'), is regarded as a 'super storm condition' (*i.e.*, 2.54). For this condition measured signals of incident waves at the toe of the dike have been used as input for the wave overtopping computations but also output from the numerical wave propagation model TRITON has been used as input. In contrast to previous computations, these computations have been performed with the actual Petten Sea-defence with a 1: 4.5 downward slope, a 1:20 berm, a 1:3 upper slope and the crest at NAP+12.9 m.

In all computations the lower 1 : 4.5 slope of the Petten Sea-defence was extended to a depth equal to the depth of the trough between the bar and the toe of the structure. This extension to deeper water was used because the depth at the toe is so small that in some situations at this position there is no water or almost no water present for a part of the wave cycle; it would therefore be hard or impossible to place the incident wave boundary at such a position. For the most important input parameters the following values were used in all computations: Δx=0.8 m (space step), Δt=0.01 s (time-step) and f=0 (friction coefficient). The computations were performed with 500 to 1000 waves. This is considered sufficient to obtain suitable estimates of wave overtopping discharges.

4.4 Analysis of the influence of low-frequency waves

Storm conditions 'January 1995'

Table 4.1 shows the results of the wave overtopping computations for the first set of computations. The first 6 conditions concern storms with conditions that actually occurred at the Petten Sea-defence. The other 14 conditions were additional conditions that were also modelled in physical model tests. Table 4.1 shows for each condition the:

- ratio of energy in low frequencies and the total energy (LFE/TE),
- wave overtopping discharge with the actual measured signal at the toe of the dike,
- wave overtopping discharge with measured signal but without the low-frequency waves *(i.e.*, filtered signals),
- ratio of wave overtopping discharge for the computations with and without low-frequency energy.

From Table 4.1 it can be observed that:

- the amount of low-frequency energy is on average 22% of the total energy,
- this resulted in an increase in wave overtopping discharges with on average a factor 1.8, with a maximum observed factor of 4.6,
- conditions with a high water level (NAP+4.7 m) resulted in a relatively low amount of low-frequency energy; for these conditions a decrease of the mean wave overtopping discharge due to the influence of low-frequency waves has been observed; the reason why this can occur remains unclear,
- all conditions that resemble storms that occurred at the Petten Sea-defence in 1995 (conditions 1-6) resulted in an increase of the mean wave overtopping discharge due to the influence of low-frequency waves,
- the conditions with the highest percentage of low-frequency energy result also in the highest increase of the mean wave overtopping discharge.

Influence of LFE on wave overtopping discharges					
No.	*SWL (NAP)*	*LFE / TE (-)*	*q with LFE (l/s/m)*	*q without LFE (l/s/m)*	*Ratio (-)*
1.01	2.10	0.25	8.1	4.6	1.8
1.02	2.04	0.30	10.9	6.1	1.8
1.03	2.24	0.29	5.2	2.4	2.2
1.04	1.66	0.45	8.2	2.8	2.9
1.05	1.60	0.27	4.0	1.8	2.2
1.06	2.04	0.25	9.1	4.4	2.1
2.11	2.10	0.11	1.7	2.6	0.7
2.13	2.10	0.22	0.6	0.3	1.7
2.15	2.10	0.35	0.4	0.1	2.9
2.21	4.70	0.02	3.1	4.2	0.7
2.23	4.70	0.07	2.4	4.0	0.6
2.25	4.70	0.11	1.5	2.2	0.7
2.31	2.10	0.15	0.5	0.5	1.0
2.41	4.70	0.03	1.7	1.8	0.9
2.51	4.70	0.09	1.6	4.2	0.4
2.54	4.70	0.10	6.0	5.2	1.2
2.61	1.30	0.30	1.6	0.6	2.7
2.71	2.10	0.27	0.5	0.2	3.1
2.72	2.10	0.38	1.4	0.3	4.6
2.73	2.10	0.33	0.4	0.2	2.7
AVERAGE		0.22			1.8
LFE: Low-frequency energy (0.01 Hz < f < 0.04 Hz) TE: Total energy (0.01 Hz < f < 0.5 Hz) For more information on the wave conditions see Van Gent (1999).					

Table 4.1 Computed contribution of low-frequency energy to wave overtopping discharges ('January 1995').

To illustrate the last finding, Figure 4.1 shows the factor of increase in wave overtopping discharge as function of the ratio of low-frequency energy and the total energy. In this figure also a trend line for this factor is shown: $f_{LFE} = 1 + 16\ (\mathrm{LFE/TE})^2$ for LFE/TE<0.5, which however does not account for the decrease in wave overtopping discharge that has been observed for low ratios of LFE/TE.

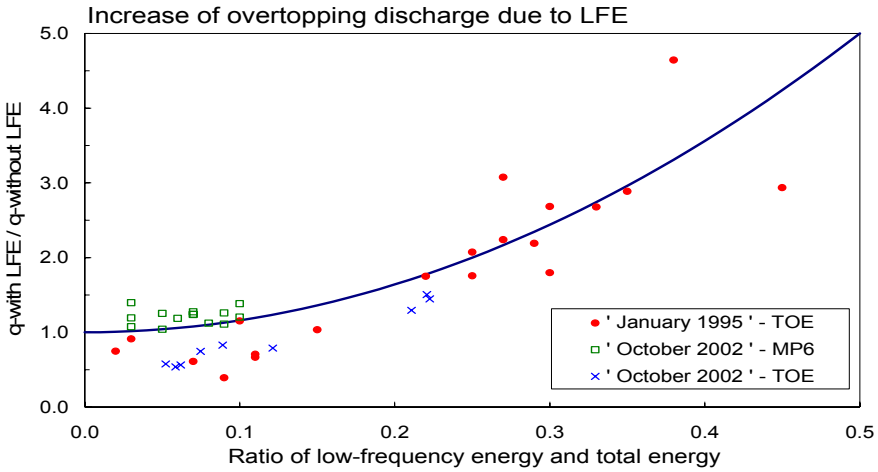

Figure 4.1 Increase of mean wave overtopping discharge as function of the ratio of low-frequency energy and total energy.

Figure 4.1 illustrates that if the amount of low-frequency energy is significant (*i.e.*, higher than about 20% of the total energy), the influence on wave overtopping discharges becomes also significant.

Storm conditions 'October 2002'

Table 4.2 shows the results of the wave overtopping computations for the second set of computations; here measured signals at MP6 have been used as input for the wave overtopping computations. Table 4.2 shows the same information as Table 4.1. The conditions shown in Table 4.2 concern however a much lower ratio of energy in low frequencies and the total energy (LFE/TE), *i.e.* lower than 10%.

From Table 4.2 it can be observed that the amount of low-frequency energy is on average 5% of the total energy and that this resulted in an increase in wave overtopping discharges with on average a factor 1.2, with a maximum observed factor of 1.4.

Influence of LFE on wave overtopping discharges (measured signals at MP6)					
No.	*SWL*	*LFE / TE*	*q with LFE*	*q without LFE*	*Ratio*
	(NAP)	*(-)*	*(l/s/m)*	*(l/s/m)*	*(-)*
1	-0.74	0.05	1.3	1.1	1.2
4	-0.52	0.06	2.2	1.7	1.3
5	0.93	0.03	0.8	0.6	1.4
6	0.56	0.08	2.3	1.7	1.4
7	1.77	0.05	3.6	3.5	1.0
8	0.23	0.07	2.7	2.4	1.1
9	1.34	0.03	1.6	1.5	1.1
11	0.77	0.05	2.0	1.6	1.2
12	1.32	0.07	6.8	5.7	1.2
13	2.21	0.06	3.0	2.5	1.2
14	0.68	0.07	5.8	5.2	1.1
15	1.20	0.04	3.8	3.1	1.3
16	-0.37	0.06	2.5	2.0	1.3
17	0.89	0.02	2.4	2.0	1.2
AVERAGE		0.05			1.2
LFE: Low-frequency energy (0.01 Hz < f < 0.04 Hz) TE: Total energy (0.01 Hz < f < 0.5 Hz)					

Table 4.2 Computed contribution of low-frequency energy (measured at MP6) to wave overtopping discharges ('October 2002').

Figure 4.1 shows the factor of increase in wave overtopping discharge as function of the ratio of low-frequency energy and the total energy. In this figure also a trend line for this factor is shown. Based on data from 'January 1995' Figure 4.1 shows that for a low amount of low-frequency energy (LFE/TE<10%) no systematic increase in wave overtopping discharge is observed. The data from 'October 2002' confirms this. Most computational results from 'October 2002' are above the trend line. Figure 4.1 illustrates that if the amount of low-frequency energy is not significant (*i.e.*, lower than about 10% of the total energy), the influence on wave overtopping discharges is also not significant.

It should be noted that the signals that have been obtained from the field measurements (MP6) are signals with surface elevations including reflected waves. Since the reflection of low-frequency waves is normally higher than the reflection of short waves, the ratio of low-frequency energy and total energy of the incident waves is most likely lower than those for the signals of surface elevations. This indicates that the applied ratio of low-frequency energy and total wave energy for the signals from field measurements are overestimated. Nevertheless, the computed dependency on this ratio (see 'open squares' in Figure 4.1) is small for the signals from the field measurements because the ratio of low-frequency energy and total energy is small; the curve in Figure 4.1 would not be influenced by this aspects.

Table 4.3 shows the results of the wave overtopping computations for the second set of computations. Now, the wave propagation model TRITON provided the signals at the toe of the dike. These were used as input for the wave overtopping computations. Table 4.3 shows again the same information as Tables 4.1 and 4.2.

From Table 4.3 it can be observed that the amount of low-frequency energy at the toe of the dike is on average 12% of the total energy. For the conditions with a relatively low percentage of low-frequency energy it was found that the mean wave overtopping discharge decreases due to low-frequency energy. Again for conditions with a relatively high percentage of low-frequency energy a relatively large increase of the mean wave overtopping discharge is observed, with a maximum observed factor of 1.5.

Influence of LFE on wave overtopping discharges (computed signals at TOE)					
No.	*SWL*	*LFE / TE*	*q with LFE*	*q without LFE*	*Ratio*
	(NAP)	*(-)*	*(l/s/m)*	*(l/s/m)*	*(-)*
1	-0.74	0.22	5.7	3.8	1.5
5	0.93	0.05	1.0	1.7	0.6
7	1.77	0.09	14.0	16.9	0.8
8	0.23	0.22	19.5	13.5	1.4
9	1.34	0.06	2.9	5.1	0.6
10	-0.37	0.21	6.2	4.8	1.3
11	0.77	0.12	8.8	11.2	0.8
13	2.21	0.06	6.8	12.7	0.5
17	0.89	0.07	3.8	5.1	0.7
AVERAGE		0.12			0.9
LFE: Low-frequency energy (0.01 Hz < f < 0.04 Hz) TE: Total energy (0.01 Hz < f < 0.5 Hz)					

Table 4.3 Computed contribution of low-frequency energy (computed at the toe) to wave overtopping discharges ('October 2002').

Figure 4.1 shows the factor of increase in wave overtopping discharge as function of the ratio of low-frequency energy and the total energy. In this figure also a trend line for this factor is shown based on data from 'January 1995'. Figure 4.1 shows that for a low amount of low-frequency energy (LFE/TE<10%) no systematic increase in wave overtopping discharge is observed. The computations with TRITON-output at the toe of the dike as input for the wave overtopping computations for 'October 2002' confirm this. These computational results are all below the trend line obtained from 'January 1995' results.

Super storm condition

One of the conditions tested in the model tests mentioned earlier ('January 1995') is regarded as a 'super storm condition' (*i.e.*, 2.54). Using measured signals as input for the numerical model ODIFLOCS resulted in 2.5 l/s/m and 1.8 l/s/m for the signals with and without low-frequency energy respectively. Thus, for this super storm condition an increase of 40% was found. Using signals computed with the model TRITON (which overestimated the significant wave height at the toe for this condition by a factor of about 1.1) resulted in 11.9 l/s/m and 11.4 l/s/m for the signals with and without low-frequency energy respectively. Thus, for this super storm condition an increase of only 4% was found.

4.5 Discussion of results

The conditions studied here indicate that:

- for the storm conditions of 'January 1995', with signals obtained from physical model tests, the amount of low-frequency energy is on average about 20% of the total energy; this resulted in an increase in wave overtopping discharges with on average a factor 1.8, with a maximum observed factor of 4.6. Conditions with a high water level (NAP+4.7 m) resulted in a relatively low amount of low-frequency energy; for these conditions a decrease of the mean wave overtopping discharge due to the influence of low-frequency waves has been observed. All conditions that resemble storms that occurred at the Petten Sea-defence in 1995 resulted in an increase of the mean wave overtopping discharge due to the influence of low-frequency waves.
- for the storm conditions of 'October 2002', with signals obtained from field measurements at MP6, the amount of low-frequency energy is on average about 6% of the total energy; this resulted in an increase in wave overtopping discharges with on average a factor 1.2, with a maximum observed factor of 1.4. For a number of conditions with a high water level a reduction in wave overtopping discharge has been observed.
- for the storm conditions of 'October 2002', with signals obtained from numerical model computations at the toe, the amount of low-frequency energy is on average about 12% of the total energy; this resulted in a decrease of wave overtopping discharges for conditions with a relatively low amount of low-frequency energy (<12%) and an increase in wave overtopping discharges for conditions with a somewhat higher amount of low-frequency energy (>12%), with a maximum observed factor of 1.5.
- for the storm condition regarded as a 'super storm condition', with signals obtained from physical model tests, the amount of low-frequency energy is about 10% of the total energy; this resulted in an increase in wave overtopping discharges with a factor 1.4.

In general it can be concluded that an influence of low-frequency energy on wave overtopping discharges has been observed. For one set of measurements, in which the amount of low-frequency energy is rather high (>20%), the increase in wave overtopping discharge increases with a larger amount of low-frequency energy. For a second set of measurements, in which the amount of low-frequency energy is rather low (<10%), the increase in wave overtopping discharge does not increase with a larger but still fairly small amount of low-frequency energy. Nevertheless, the results indicate that if the amount of low-frequency energy is higher than about 20% of the total energy, the influence on wave overtopping discharges can become significant.

In the method that has been applied for each condition two computations have been performed, one with a wave train including low-frequency energy and one with the same wave train but without low-frequency energy. This means that the wave train without low-frequency waves contains the original short waves, while the low frequencies are filtered out. However, there may still be effects of low-frequency waves on these short waves. For instance, if a high short wave propagates in shallow water on the crest of a low-frequency wave this may cause that this short wave does not break due to the temporarily high water level. If the low-frequency wave is filtered away, the same high short wave is present in the time-signal. However, without the low-frequency wave this high short wave might normally break because it propagates in shallower water. This means that higher short waves can occur in the obtained wave trains (after filtering away low-frequency waves), higher than those which would in reality be possible. Therefore, the method followed here may result in too high short waves and an overestimate of wave overtopping discharges. This may result in an underestimate of the possible influence of low-frequency waves.

5 Conclusions and recommendations

Based on the investigations described in this report the following conclusions and recommendations can be given:

Conclusions:

- Field measurements during the storm period of October 25 to 28, 2002, have been analysed on a few aspects. One of them is wave reflection. It appeared that at the location MP 17 (about 280 m from the dike) measured wave reflection is on average 61% for low-frequency energy (between 0.01 Hz and 0.04 Hz). For short waves the reflection coefficients based on energy are on average 23% (around the peaks of the wave energy spectra).
- Field measurements showed that the amount of low-frequency energy, as well as the percentage of the total wave energy, increases from an average of 1% at MP3 (about 610 m from the dike) to an average of 5% of the total energy, and a maximum of 8%, at MP6 (about 125 m from the dike); 5% in energy means that the H_{m0} based on the energy in the low frequencies is 22% of the wave height based on all energy.
- The amount of low-frequency energy computed with the numerical model TRITON is higher than measured at MP6. The model can also provide estimates of low-frequency energy at the toe of the dike. On average the model provided estimates of low-frequency energy of 12% of the total energy at the toe of the dike. A validation of the model TRITON with respect to the ratio of energy in low-frequency waves and the total amount of energy, showed accurate estimates.
- The numerical model ODIFLOCS has been used to analyse the possible influence of low-frequency waves on mean wave overtopping discharges. An influence of low-frequency energy on wave overtopping discharges has been observed. For conditions in which the amount of energy in low-frequency waves is small, mean wave overtopping discharges hardly increase due to low-frequency waves. Even a reduction in mean overtopping discharge has been observed for a number of conditions. For conditions in which the amount of energy in low-frequency waves is significant, the influence on mean wave overtopping discharges is also significant; a factor of almost 5 has been observed. For the analysed storm period 'October 2002', a much lower factor was found (up to 1.4). Also for a condition considered as a 'super storm condition' a factor of 1.4 was found. A factor of 1.4 would have a rather small effect on the required crest elevation due to the influence of low-frequency energy. An estimate of the factor with which mean overtopping discharges are increased due to the presence of low-frequency energy (LFE) is given: $f_{LFE} = 1 + 16\ (\mathrm{LFE/TE})^2$ for $\mathrm{LFE/TE}<0.5$.
- The method applied here may lead to underestimates of the influence of low-frequency waves. This is due to the method applied to filter the low-frequency waves out of the measured and computed wave trains, which may lead to overestimates of the wave height of short waves in the absence of low-frequency waves.

Recommendations:

- Since wave reflection, especially for low-frequency waves, appears to be significant, it is recommended to study the influence of wave reflection on the wave conditions on the foreshore.
- The analysis of measured low-frequency waves leads to results that cannot always be explained completely. Therefore, it is advised to study in more detail the measured low-frequency waves. Also energy in frequencies smaller than 0.01 Hz could be part of additional investigations, as well as the influence of (changes in) the bathymetry.
- The study performed here was partly based on 1D computations with a numerical wave propagation model. This 1D modelling does not account for effects of directional spreading on the amount of energy in low-frequency waves. Since directional spreading may lead to a lower amount of low-frequency energy, it is recommended to study the influence of directional spreading on the amount of low-frequency energy.
- It is recommended to improve the modelling of wave propagation and to study the generation of low-frequency waves in shallow water. For some cases accurate results have been obtained, but improvements, especially for 2D situations, are desirable. It is also recommended to include the modelling of the wave motion on the dike in the same model as for wave propagation (TRITON); this could solve inaccuracies related to the transition of the model for the foreshore (TRITON) and the model for the dike (ODIFLOCS).
- The storm period October 25-28, 2002, showed a rather low amount of energy in low-frequency waves (*i.e.*, much lower than in the storms that were measured in the wave flume with conditions from 'January 1995'). Therefore, it is recommended to keep the field measurement site operational to enable the analysis of low-frequency waves for more severe storms.
- The analysis in this report showed that there is an influence of low-frequency waves on mean wave overtopping discharges. For conditions with a relatively large amount of low-frequency energy this influence is significant. Therefore, it is recommended to take the effects of low-frequency energy into account in crest level design of dikes.

Acknowledgements

This study contributes to the analysis of phenomena that are important for wave overtopping. This is a topic of interest for the EU project CLASH (contract EVK-2001-00064).

References

Borsboom, M.J.A., N. Doorn, J. Groeneweg and M.R.A. van Gent (2000), *A Boussinesq-type wave model that conserves both mass and momentum*, ASCE, Proc. ICCE 2000, Sydney, pp.148-161.

Borsboom, M.J.A., J. Groeneweg, N. Doorn and M.R.A. van Gent (2001-a), *Near-shore wave simulation with a Boussinesq-type wave model including wave breaking,* ASCE, Proc. Coastal Dynamics 2001, Lund, Sweden, pp.759-768.

Borsboom, M.J.A., J. Groeneweg, N. Doorn and M.R.A. van Gent (2001-b), *Flexible boundary conditions for a Boussinesq-type wave mode,* ASCE, Proc. Waves 2001, San Francisco, pp. 884-993.

De Haas, P.C.A., D.C. Rijks, B.G. Ruessink, J.A. Roelvink, A.J.H.M. Reniers, M.R.A. van Gent (1999), *Onderzoek naar lange golven bij Petten (in Dutch); Investigations on long waves at Petten*, Report by University Utrecht and Delft Hydraulics, Report H3345-January 1999, Delft.

De Kruif, A.C. (2000), *Stormdata of the Petten Field Site: 1995-2000,* RIKZ Report RIKZ/OS/2000/34X-September 2000, The Hague, The Netherlands.

Groeneweg, J., N. Doorn, M.J.A. Borsboom and M.R.A. van Gent (2002), *Boussinesq-type modeling of measured wave breaking on a circular shoal*, ASCE, Proc. ICCE 2002, Cardiff, pp.495-507.

Hordijk, D. (2003), *Report on field measurements; Petten Sea defence; Stormseason 2002-2003*, Report RIKZ/OS_2003.135X by Rijkswaterstaat-RIKZ, July 2003.

Hibberd, S. and D.H. Peregrine (1979), *Surf and run-up on a beach: a uniform bore*, J. of Fluid Mechanics, Vol.95, part 2, pp.323-345.

Kennedy, A.B., Q. Chen, J.T. Kirby and R.A. Dalrymple (2000), *Boussinesq modeling of wave transformation, breaking and runup. I One Dimension,* J. of Waterway, Port, Coastal and Ocean Engrg, ASCE, Vol.126, pp.39-47.

Kobayashi, N., A.K. Otta and I. Roy (1987), *Wave reflection and run-up on rough slopes*, J. of Waterway, Port, Coastal and Ocean Engrg, ASCE, Vol.113, No.3, pp.282-298.

Mansard, E. and E. Funke (1980), *The measurement of incident and reflected spectra using a least-square method*, Proc. ICCE'80, Sydney.

Schäffer, H.A., R. Deigaard and P. Madsen (1992), *A two-dimensional surf-zone model based on the Boussinesq equations*, Proc. ICCE'92, Vol.1., pp.576-589, Venice.

Van Gent, M.R.A. (1994), *The modelling of wave action on and in coastal structures,* Coastal Engineering, Vol.22 (3-4), pp.311-339, Elsevier, Amsterdam.

Van Gent, M.R.A. (1995), *Wave interaction with permeable coastal structures*, Ph.D.-thesis, Delft University of Technology, ISBN 90-407-1182-8, Delft University Press, Delft.

Van Gent, M.R.A. (1999), *Physical model investigations on coastal structures with shallow foreshores; 2D model test on the Petten Sea-defence*, Delft Hydraulics Report H3129-July 1999, Delft.

Van Gent, M.R.A. (2001), *Wave run-up on dikes with shallow foreshores*, ASCE, Journal of Waterway, Port, Coastal and Ocean Engineering, Vol.127, No.5, Sept/Oct 2001, pp.254-262.

Van Gent, M.R.A., A.C. de Kruif and J. Murphy (2001), *Field measurements and laboratory investigations on wave propagation and wave run-up,* ASCE, Proc. Waves 2001, San Francisco, pp.734-743.

Van Gent, M.R.A. and N. Doorn (2001), *Wave propagation and wave run-up on dikes with shallow foreshores,* ASCE, Proc. Coastal Dynamics 2001, Lund, Sweden, pp.769-778.

Tables

MP3							
No	*Date*	*Time (hour)*	*LFE / TE (-)*	H_{m0} *(short)*	H_{m0} *(LFE)*	H_{m0} *(total)*	$T_{m-1,0}$ *(total)*
1	25-10-2002	2-4	0.00	1.33	0.07	1.33	7.4
2	25-10-2002	4-6	0.00	1.78	0.10	1.79	7.3
3	25-10-2002	10-12	0.00	2.43	0.15	2.43	6.2
4	25-10-2002	14-16	0.00	2.01	0.14	2.02	6.7
5	25-10-2002	18-20	0.00	2.29	0.15	2.30	6.5
6	26-10-2002	2-4	0.01	3.41	0.27	3.42	7.9
7	26-10-2002	6-8	0.01	4.33	0.33	4.35	8.0
8	26-10-2002	14-16	0.00	3.16	0.21	3.17	7.9
9	26-10-2002	18-20	0.00	2.80	0.17	2.80	7.0
10	27-10-2002	1-3	0.01	1.79	0.13	1.79	6.7
11	27-10-2002	9-11	0.01	3.34	0.24	3.35	7.5
12	27-10-2002	15-17	0.01	4.71	0.51	4.74	9.6
13	27-10-2002	20-22	0.01	6.49	0.49	6.51	9.4
14	28-10-2002	4-6	0.01	3.76	0.41	3.79	8.9
15	28-10-2002	8-10	0.03	3.32	0.55	3.36	9.3
16	28-10-2002	16-18	0.02	2.30	0.35	2.33	8.5
17	28-10-2002	20-22	0.01	2.06	0.24	2.07	7.7

These wave conditions are based on analysis of signals of surface elevations including reflected waves.
LFE: Low-frequency energy (0.01 Hz – 0.04 Hz)
TE: Total wave energy (0.01 Hz – 0.5 Hz)
NR: Not Reliable

Table T1.1 Measured storm conditions at MP3.

MP17							
No	*Date*	*Time (hour)*	*LFE / TE (-)*	H_{m0} *(short)*	H_{m0} *(LFE)*	H_{m0} *(total)*	$T_{m-1,0}$ *(total)*
1	25-10-2002	2-4	0.01	0.83	0.10	0.84	8.2
2	25-10-2002	4-6	0.01	0.71	0.07	0.71	10.2
3	25-10-2002	10-12	0.02	1.01	0.15	1.02	7.6
4	25-10-2002	14-16	0.02	1.01	0.16	1.02	8.2
5	25-10-2002	18-20	0.02	1.18	0.19	1.19	8.0
6	26-10-2002	2-4	0.04	1.29	0.25	1.31	9.6
7	26-10-2002	6-8	0.03	1.75	0.32	1.78	9.8
8	26-10-2002	14-16	0.03	1.33	0.22	1.34	9.3
9	26-10-2002	18-20	0.02	1.44	0.19	1.45	8.2
10	27-10-2002	1-3	0.02	1.06	0.14	1.07	8.1
11	27-10-2002	9-11	0.04	1.36	0.26	1.39	9.5
12	27-10-2002	15-17	0.07	1.45	0.41	1.51	12.2
13	27-10-2002	20-22	0.04	2.05	0.43	2.10	11.1
14	28-10-2002	4-6	0.04	1.56	0.33	1.59	10.6
15	28-10-2002	8-10	0.03	1.79	0.29	1.81	9.5
16	28-10-2002	16-18	0.02	1.19	0.17	1.20	8.6
17	28-10-2002	20-22	0.02	1.19	0.16	1.20	8.3

These wave conditions are based on analysis of signals of surface elevations including reflected waves.
LFE: Low-frequency energy (0.01 Hz – 0.04 Hz)
TE: Total wave energy (0.01 Hz – 0.5 Hz)
NR: Not Reliable

Table T1.2 Measured storm conditions at MP17.

MP18							
No	*Date*	*Time (hour)*	*LFE / TE (-)*	H_{m0} *(short)*	H_{m0} *(LFE)*	H_{m0} *(total)*	$T_{m-1,0}$ *(total)*
1	25-10-2002	2-4	NR	NR	NR	NR	NR
2	25-10-2002	4-6	0.01/NR	0.80/NR	0.08/NR	0.81/NR	9.7/NR
3	25-10-2002	10-12	0.02	1.06	0.14	1.07	7.3
4	25-10-2002	14-16	0.04/NR	0.47/NR	0.09/NR	0.48/NR	10.4/NR
5	25-10-2002	18-20	0.02	1.37	0.19	1.38	8.0
6	26-10-2002	2-4	0.04	1.58	0.34	1.62	9.6
7	26-10-2002	6-8	0.04/NR	2.16/NR	0.46/NR	2.21/NR	9.8/NR
8	26-10-2002	14-16	0.03/NR	1.38/NR	0.25/NR	1.40/NR	9.3/NR
9	26-10-2002	18-20	0.02	1.60	0.25	1.62	8.2
10	27-10-2002	1-3	0.03/NR	0.55/NR	0.09/NR	0.56/NR	8.1/NR
11	27-10-2002	9-11	0.04	1.63	0.33	1.66	9.5
12	27-10-2002	15-17	0.07	1.91	0.52	1.98	12.2
13	27-10-2002	20-22	0.06/NR	1.98/NR	0.50/NR	2.05/NR	11.1/NR
14	28-10-2002	4-6	0.04/NR	1.75/NR	0.37/NR	1.79/NR	11.0/NR
15	28-10-2002	8-10	0.03	1.91	0.34	1.94	9.7
16	28-10-2002	16-18	0.03/NR	0.73/NR	0.14/NR	0.75/NR	10.0/NR
17	28-10-2002	20-22	0.01	1.44	0.18	1.45	8.2

These wave conditions are based on analysis of signals of surface elevations including reflected waves.
LFE: Low-frequency energy (0.01 Hz – 0.04 Hz)
TE: Total wave energy (0.01 Hz – 0.5 Hz)
NR: Not Reliable

Table T1.3 Measured storm conditions at MP18.

MP6							
No	*Date*	*Time (hour)*	*LFE / TE (-)*	H_{m0} *(short)*	H_{m0} *(LFE)*	H_{m0} *(total)*	$T_{m-1,0}$ *(total)*
1	25-10-2002	2-4	0.05	0.48	0.11	0.50	11.4
2	25-10-2002	4-6	0.02	0.82	0.10	0.83	10.6
3	25-10-2002	10-12	0.02	0.93	0.14	0.94	8.0
4	25-10-2002	14-16	0.06	0.55	0.14	0.56	10.8
5	25-10-2002	18-20	0.03	1.14	0.19	1.16	8.8
6	26-10-2002	2-4	0.08	1.11	0.32	1.15	11.5
7	26-10-2002	6-8	0.05	1.74	0.39	1.78	10.9
8	26-10-2002	14-16	0.07	0.99	0.27	1.02	11.6
9	26-10-2002	18-20	0.03	1.37	0.25	1.40	9.3
10	27-10-2002	1-3	0.05/NR	0.69/NR	0.15/NR	0.70/NR	10.4/NR
11	27-10-2002	9-11	0.05	1.20	0.27	1.23	10.6
12	27-10-2002	15-17	0.07	1.67	0.48	1.74	13.5
13	27-10-2002	20-22	0.06	1.87	0.47	1.93	12.5
14	28-10-2002	4-6	0.07	1.29	0.36	1.34	12.4
15	28-10-2002	8-10	0.04	1.50	0.32	1.54	10.8
16	28-10-2002	16-18	0.06	0.76	0.19	0.78	11.2
17	28-10-2002	20-22	0.02	1.19	0.18	1.20	8.9

These wave conditions are based on analysis of signals of surface elevations including reflected waves.
LFE: Low-frequency energy (0.01 Hz – 0.04 Hz)
TE: Total wave energy (0.01 Hz – 0.5 Hz)
NR: Not Reliable

Table T1.4 Measured storm conditions at MP6.

Validation of LFE computed by TRITON					
No.	*SWL*	*TE*	*LFE / TE*	*LFE / TE*	*DIFFERENCE*
	(NAP)	*COMP/MEAS*	*MEASURED*	*COMPUTED*	*%*
1	-0.74	1.8	0.01	0.02	0.2
5	0.93	2.6	0.02	0.01	-1.0
7	1.77	3.4	0.03	0.03	-0.1
8	0.23	2.2	0.03	0.04	1.2
9	1.34	2.7	0.02	0.02	0.3
10	-0.37	1.8	0.02	0.03	1.0
11	0.77	3.6	0.04	0.03	-0.7
13	2.21	5.2	0.04	0.02	-1.9
17	0.89	2.1	0.02	0.02	0.7
AVERAGE		2.8	0.0252	0.0250	0.0
LFE: Low-frequency energy (0.01 Hz < f < 0.04 Hz) TE: Total energy (0.01 Hz < f < 0.5 Hz) NR: Not Reliable					

Table T2.1 Measured and computed wave energy in low-frequency waves at MP17 (‘October 2002’).

Validation of LFE computed by TRITON					
No.	*SWL*	*TE*	*LFE / TE*	*LFE / TE*	*DIFFERENCE*
	(NAP)	*COMP/MEAS*	*MEASURED*	*COMPUTED*	*%*
1	-0.74	NR	NR	0.02	NR
5	0.93	2.0	0.02	0.02	0.3
7	1.77	NR	NR	0.05	NR
8	0.23	NR	NR	0.05	NR
9	1.34	2.3	0.02	0.03	0.7
10	-0.37	NR	NR	0.04	NR
11	0.77	2.7	0.04	0.04	0.3
13	2.21	NR	NR	0.04	NR
17	0.89	1.6	0.01	0.03	1.7
AVERAGE		2.2	0.02	0.03	0.8
LFE: Low-frequency energy (0.01 Hz < f < 0.04 Hz) TE: Total energy (0.01 Hz < f < 0.5 Hz) NR: Not Reliable					

Table T2.2 Measured and computed wave energy in low-frequency waves at MP18 (‘October 2002’).

Validation of LFE computed by TRITON					
No.	*SWL*	*TE*	*LFE / TE*	*LFE / TE*	*DIFFERENCE*
	(NAP)	*COMP/MEAS*	*MEASURED*	*COMPUTED*	*%*
1	-0.74	6.5	0.05	0.03	-2.1
5	0.93	3.1	0.03	0.03	0.0
7	1.77	3.8	0.05	0.05	0.5
8	0.23	4.7	0.07	0.06	-0.8
9	1.34	3.3	0.03	0.04	0.5
10	-0.37	5.0	0.05	0.05	0.0
11	0.77	5.3	0.05	0.05	0.5
13	2.21	5.8	0.06	0.04	-1.6
17	0.89	2.4	0.02	0.04	1.5
AVERAGE		4.4	0.04	0.04	-0.2
LFE: Low-frequency energy (0.01 Hz < f < 0.04 Hz) TE: Total energy (0.01 Hz < f < 0.5 Hz) NR: Not Reliable					

Table T2.3 Measured and computed wave energy in low-frequency waves at MP6 (‘October 2002’).

Figures

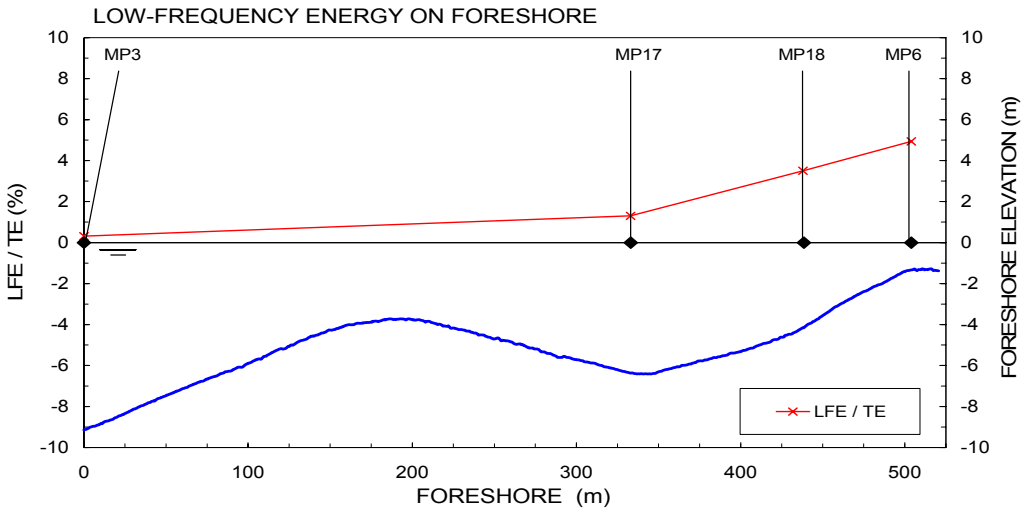

Figure F1.1 Percentage of low-frequency energy at positions on the foreshore (condition 1).

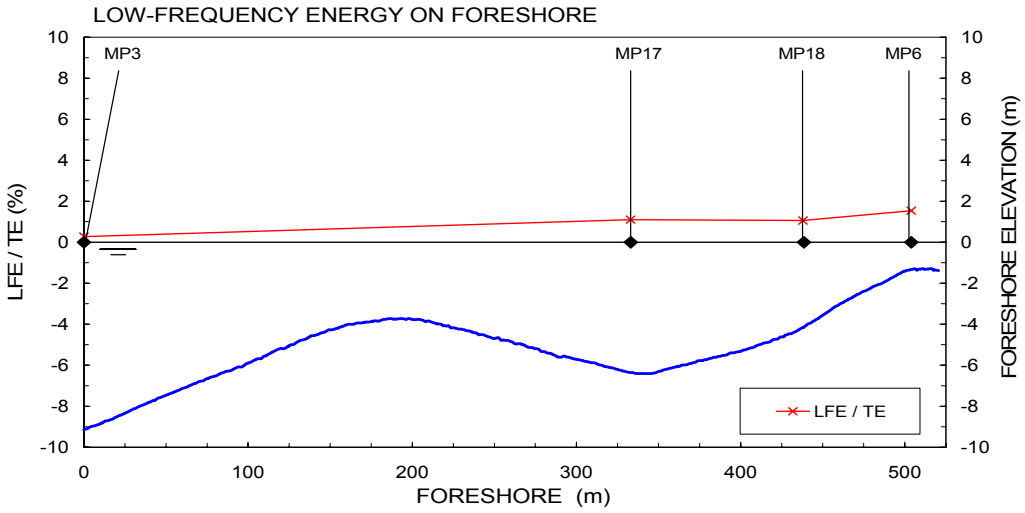

Figure F1.2 Percentage of low-frequency energy at positions on the foreshore (condition 2).

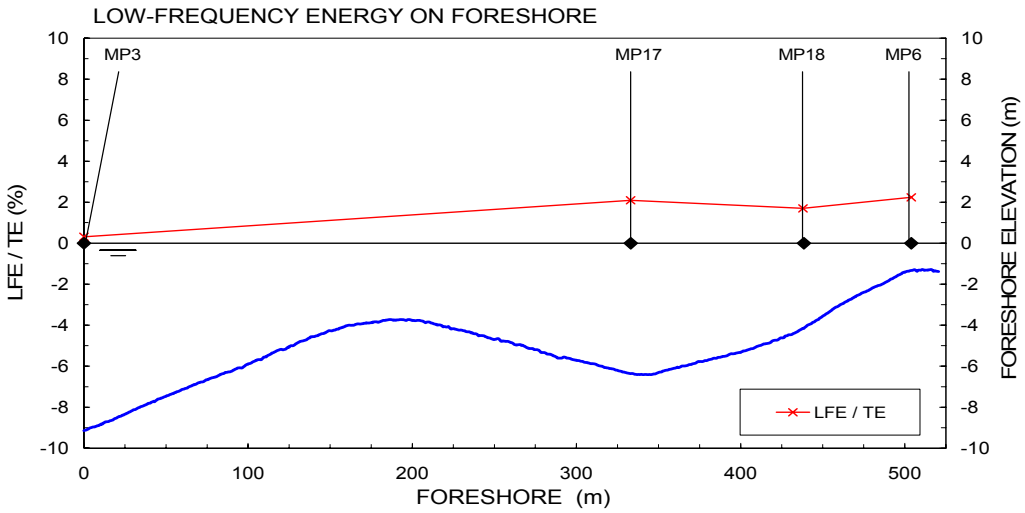

Figure F1.3 Percentage of low-frequency energy at positions on the foreshore (condition 3).

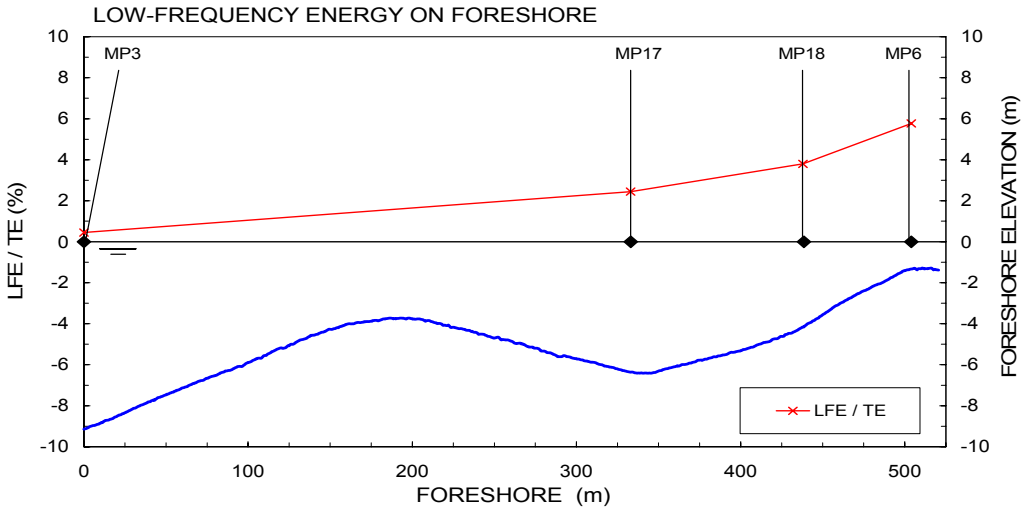

Figure F1.4 Percentage of low-frequency energy at positions on the foreshore (condition 4).

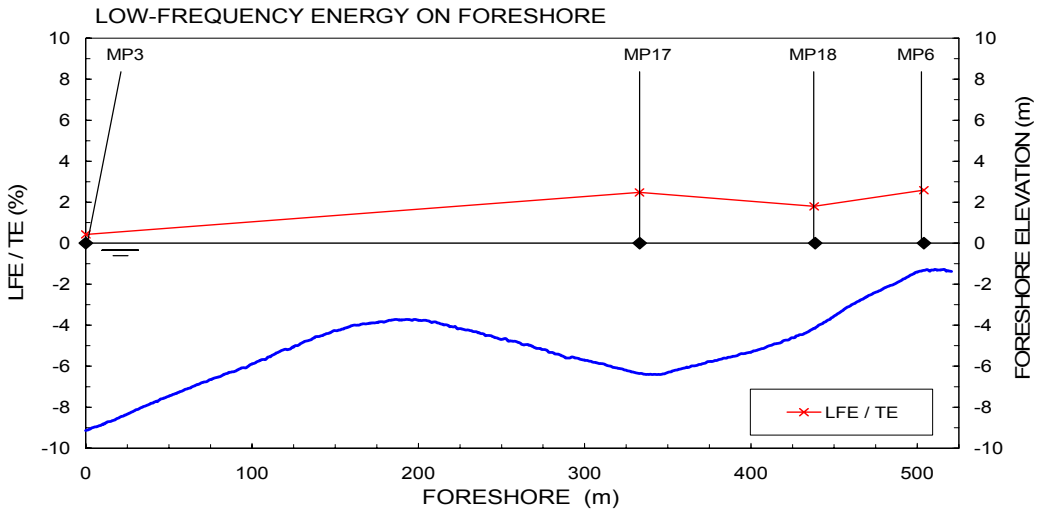

Figure F1.5 Percentage of low-frequency energy at positions on the foreshore (condition 5).

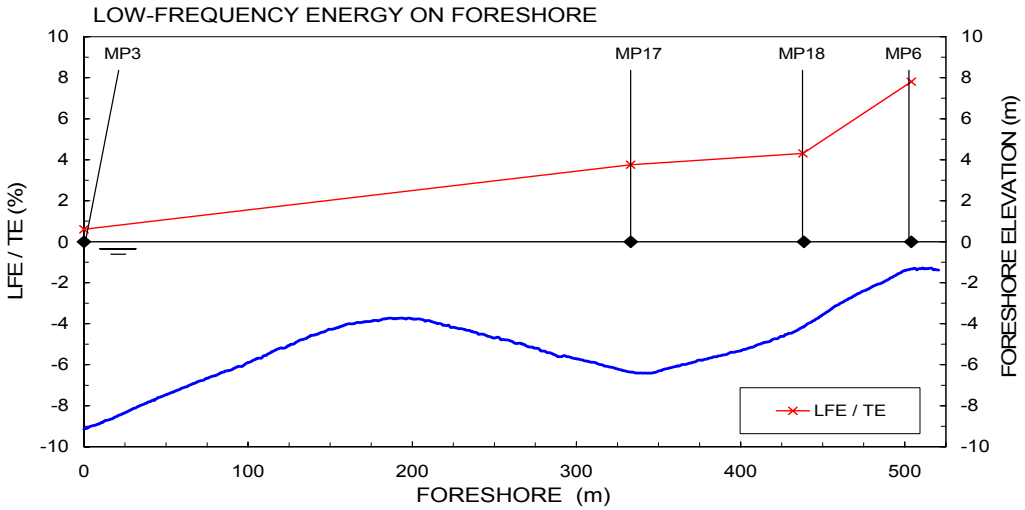

Figure F1.6 Percentage of low-frequency energy at positions on the foreshore (condition 6).

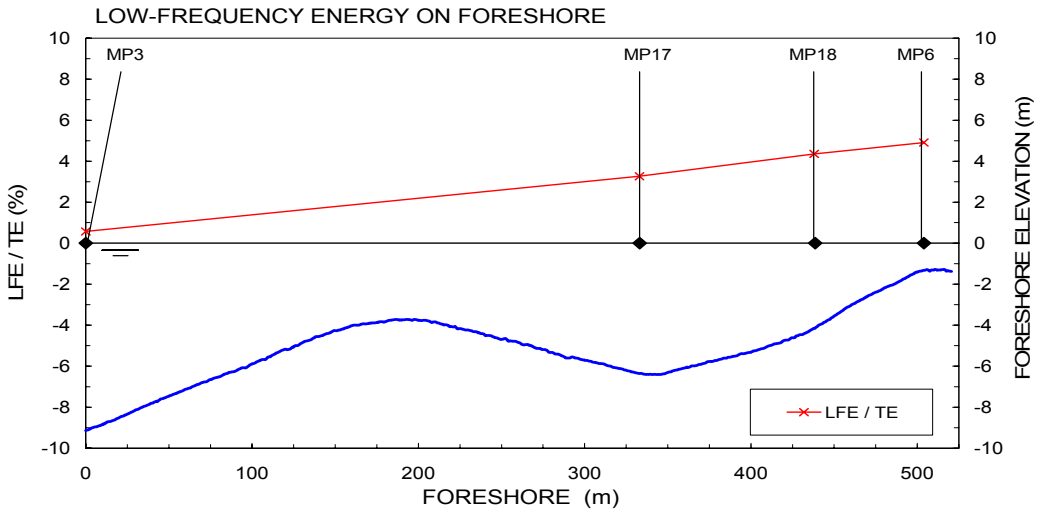

Figure F1.7 Percentage of low-frequency energy at positions on the foreshore (condition 7).

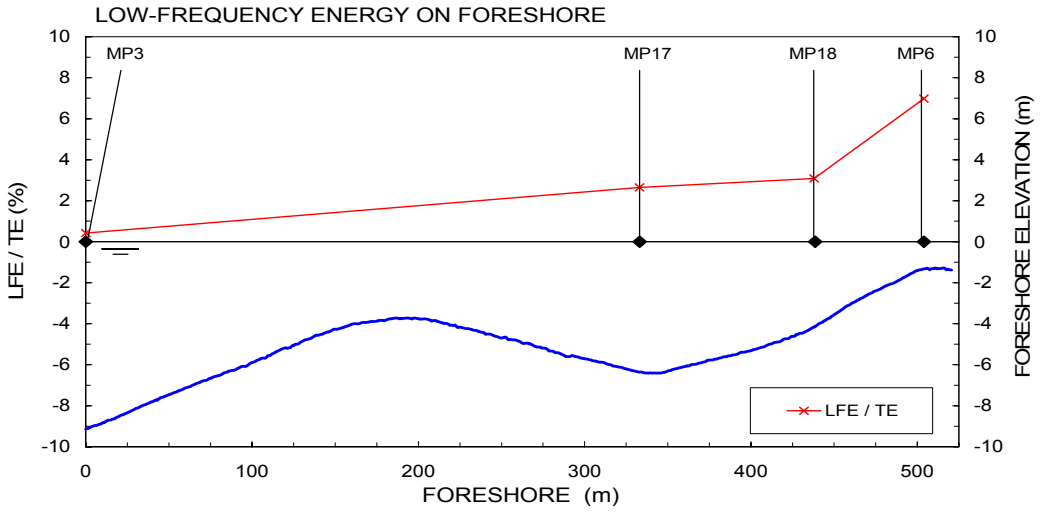

Figure F1.8 Percentage of low-frequency energy at positions on the foreshore (condition 8).

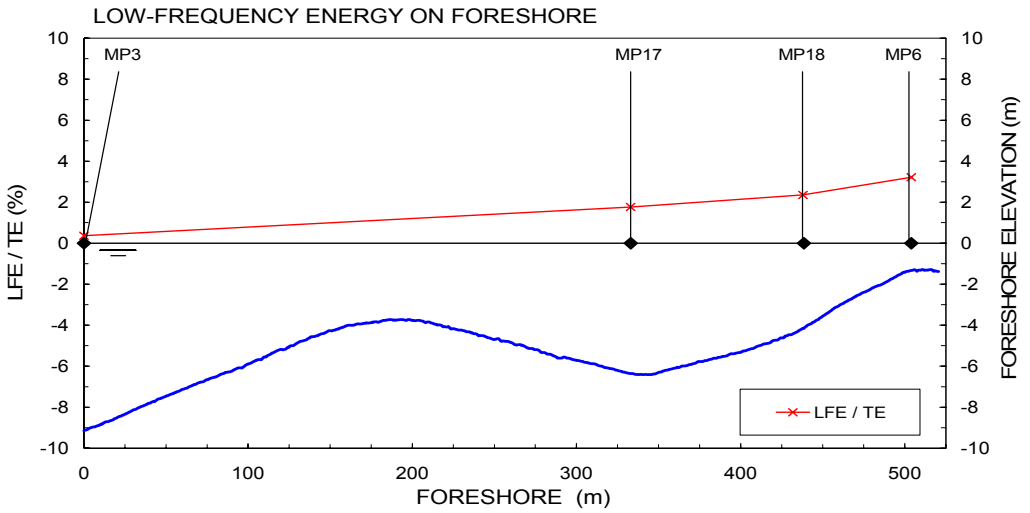

Figure F1.9 Percentage of low-frequency energy at positions on the foreshore (condition 9).

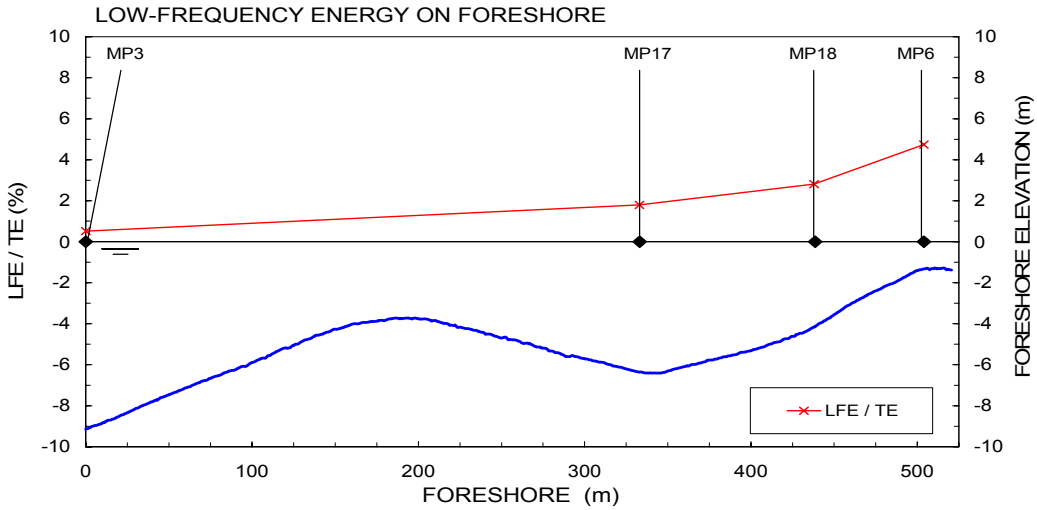

Figure F1.10 Percentage of low-frequency energy at positions on the foreshore (condition 10).

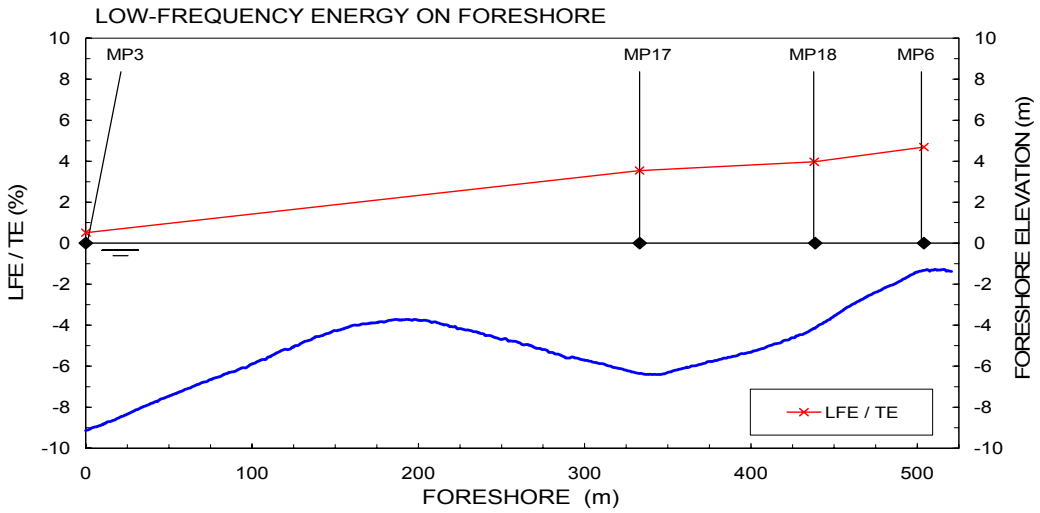

Figure F1.11 Percentage of low-frequency energy at positions on the foreshore (condition 11).

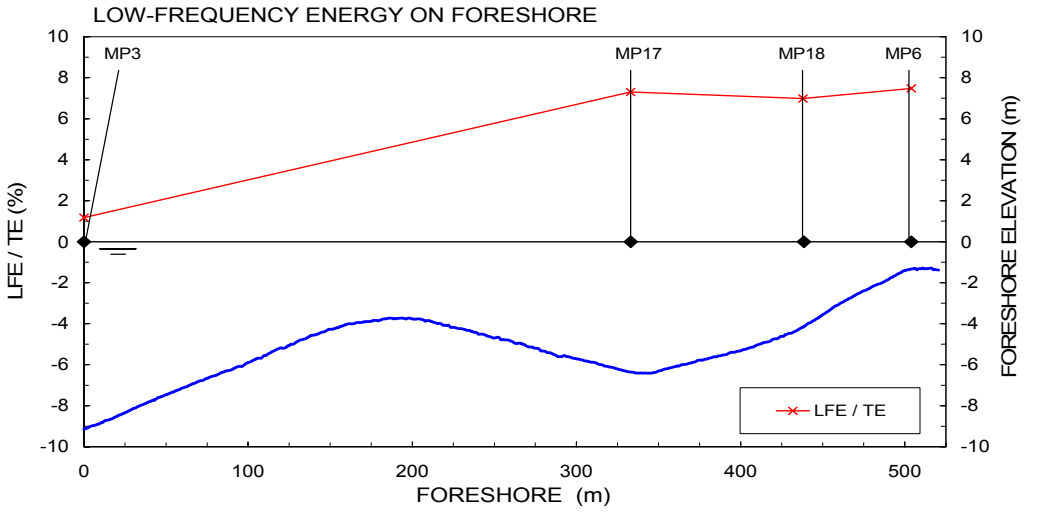

Figure F1.12 Percentage of low-frequency energy at positions on the foreshore (condition 12).

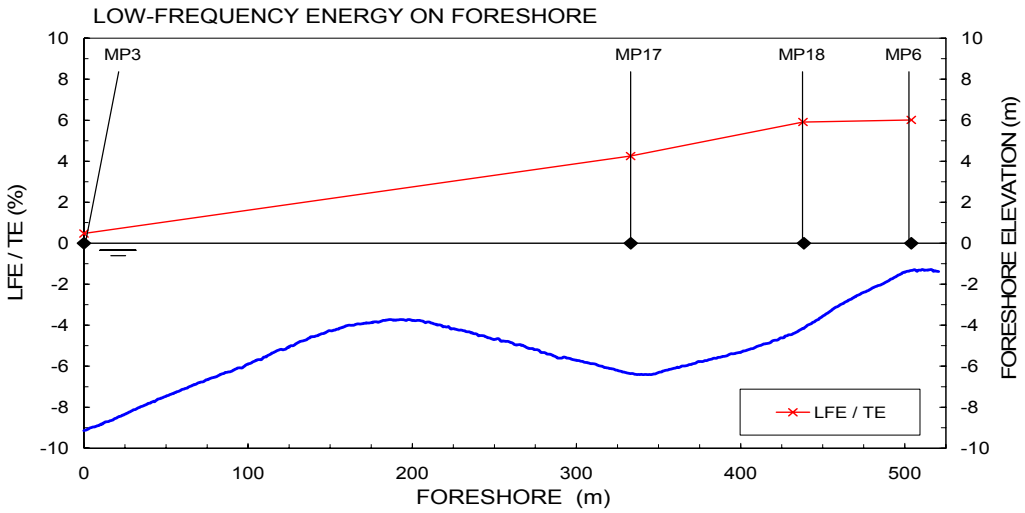

Figure F1.13 Percentage of low-frequency energy at positions on the foreshore (condition 13).

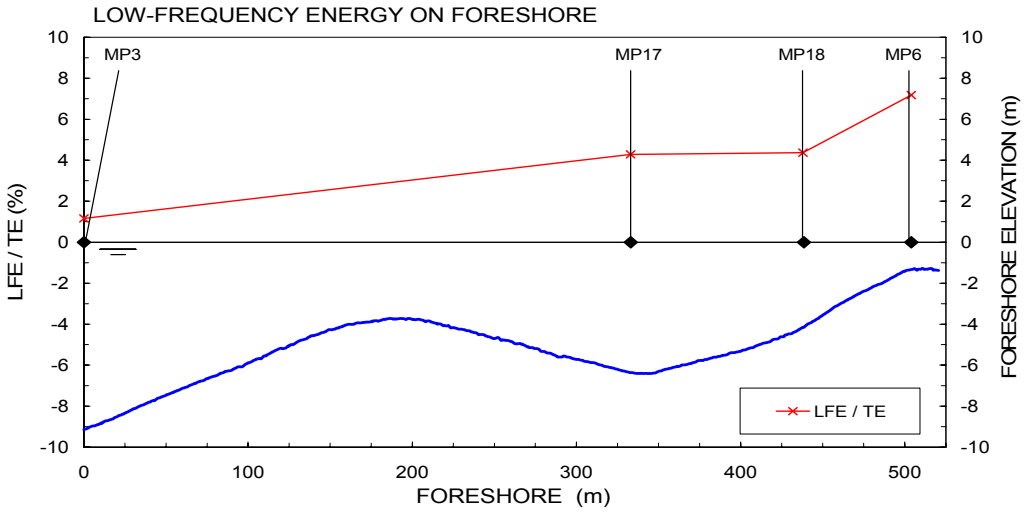

Figure F1.14 Percentage of low-frequency energy at positions on the foreshore (condition 14).

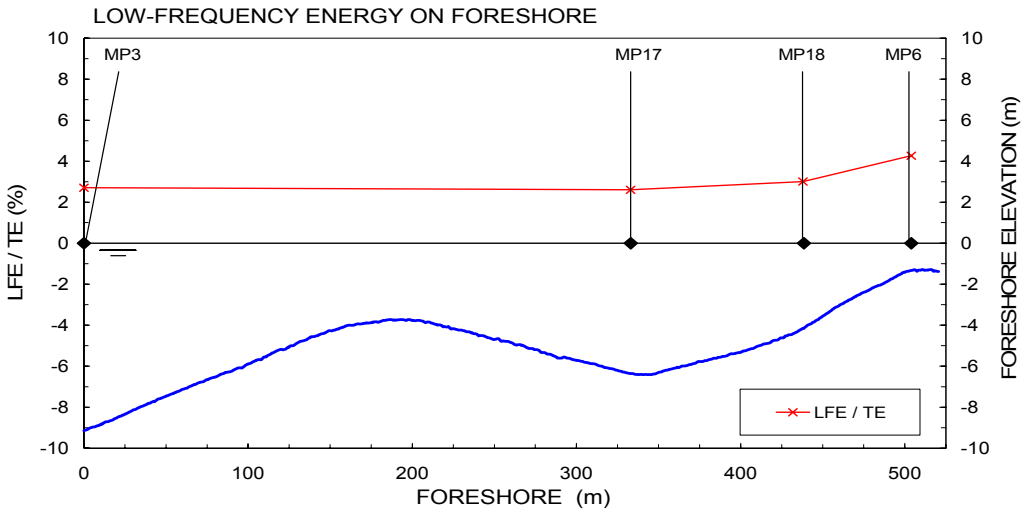

Figure F1.15 Percentage of low-frequency energy at positions on the foreshore (condition 15).

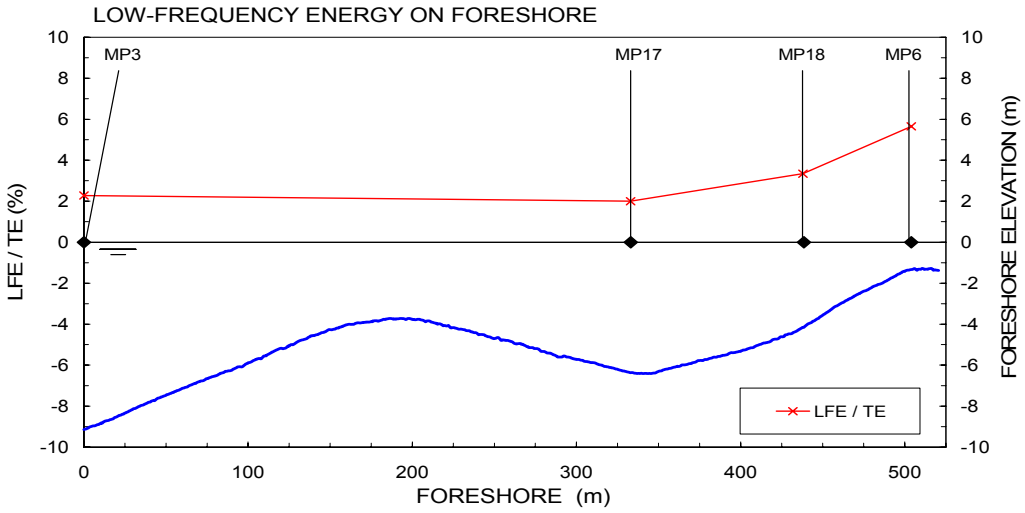

Figure F1.16 Percentage of low-frequency energy at positions on the foreshore (condition 16).

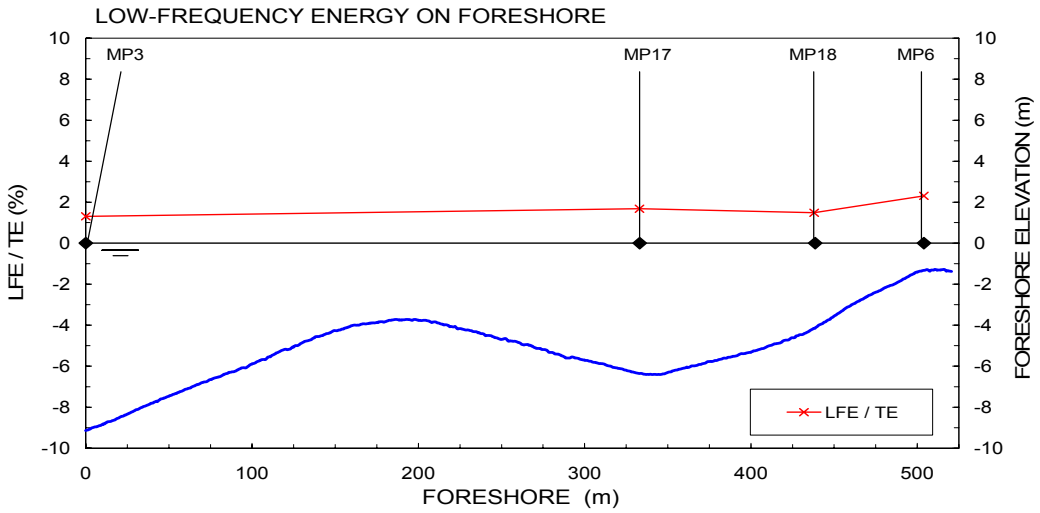

Figure F1.17 Percentage of low-frequency energy at positions on the foreshore (condition 17).

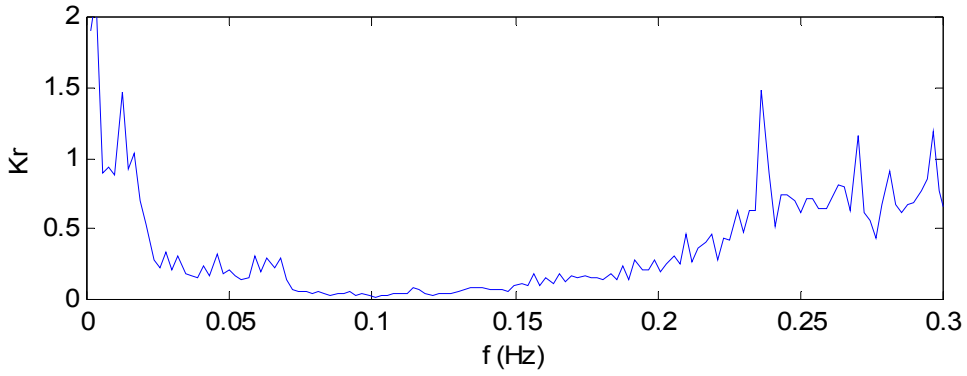

Figure F2.1 Wave reflection as function of wave frequency (condition 1).

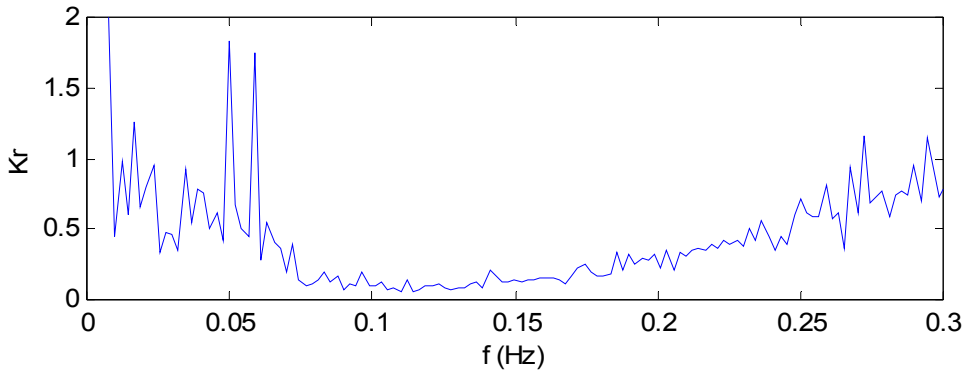

Figure F2.2 Wave reflection as function of wave frequency (condition 2).

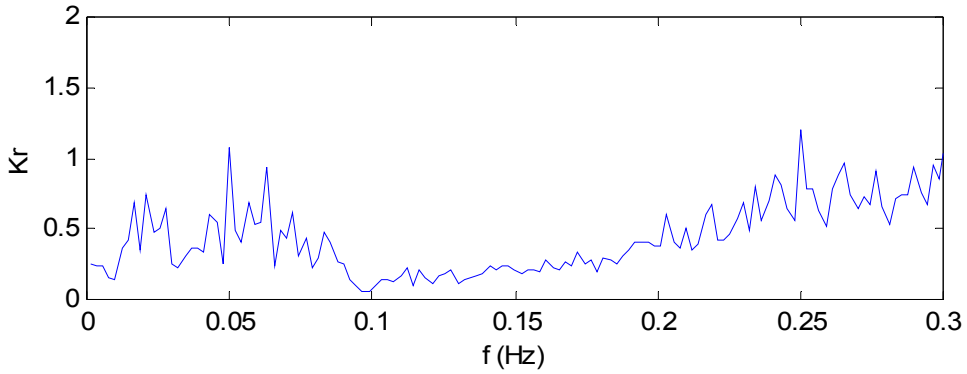

Figure F2.3 Wave reflection as function of wave frequency (condition 3).

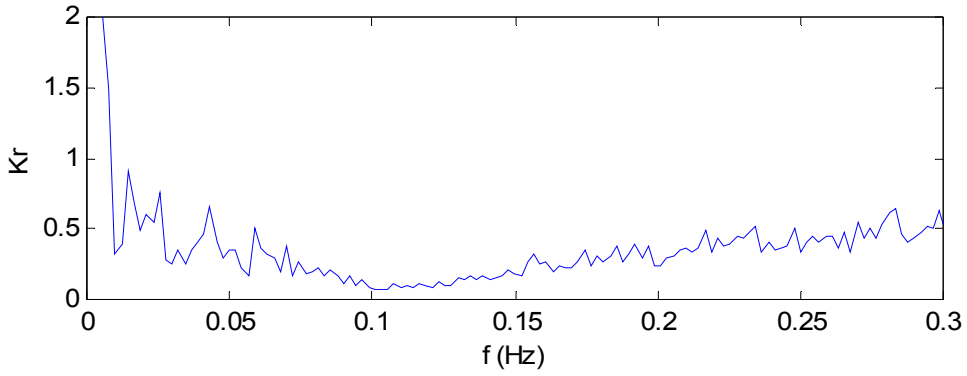

Figure F2.4 Wave reflection as function of wave frequency (condition 4).

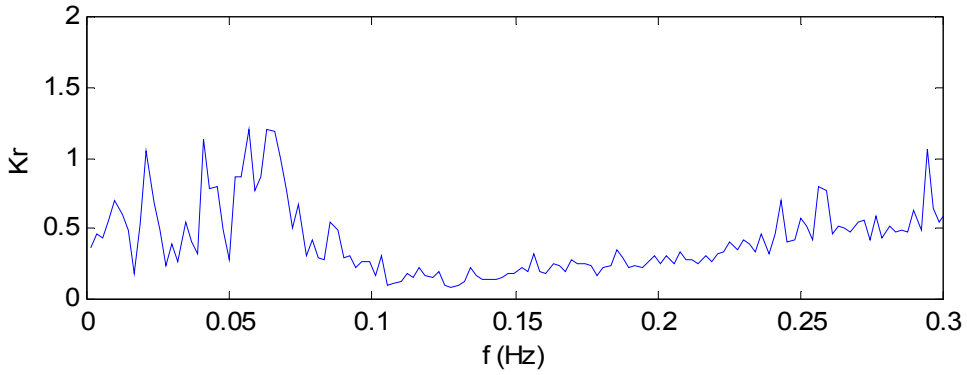

Figure F2.5 Wave reflection as function of wave frequency (condition 5).

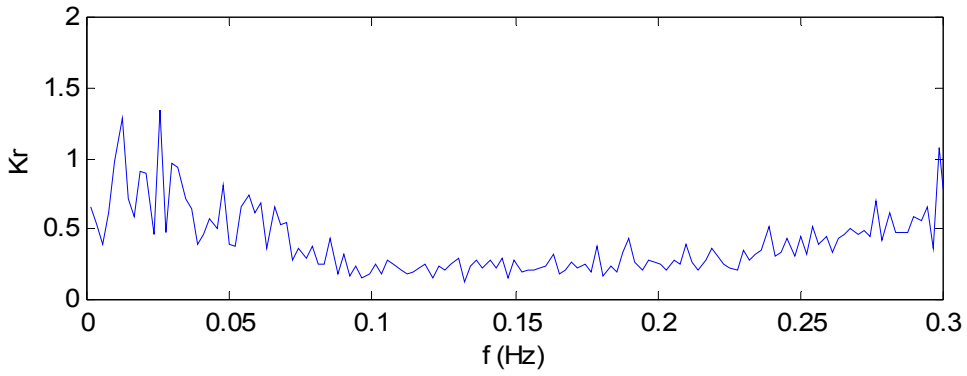

Figure F2.6 Wave reflection as function of wave frequency (condition 6).

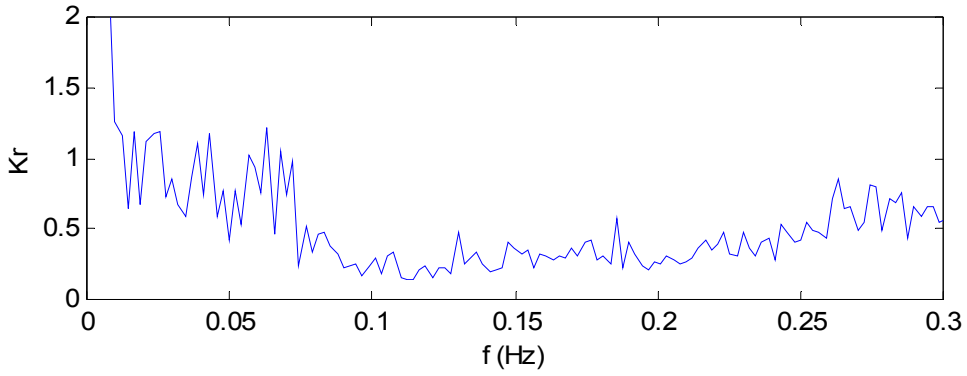

Figure F2.7 Wave reflection as function of wave frequency (condition 7).

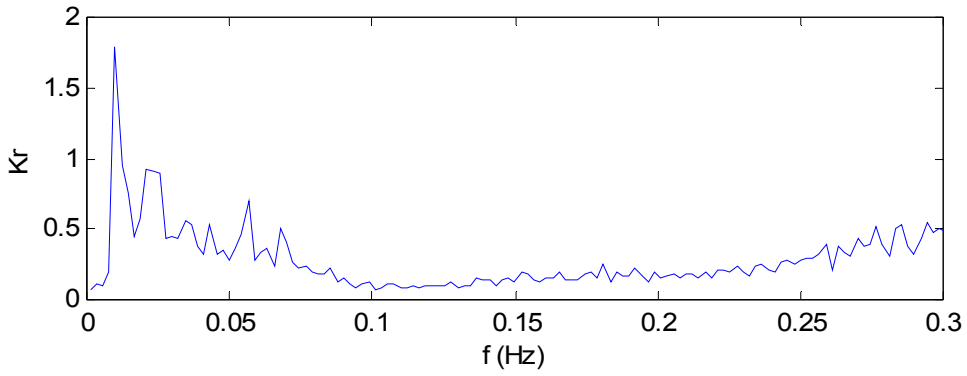

Figure F2.8 Wave reflection as function of wave frequency (condition 8).

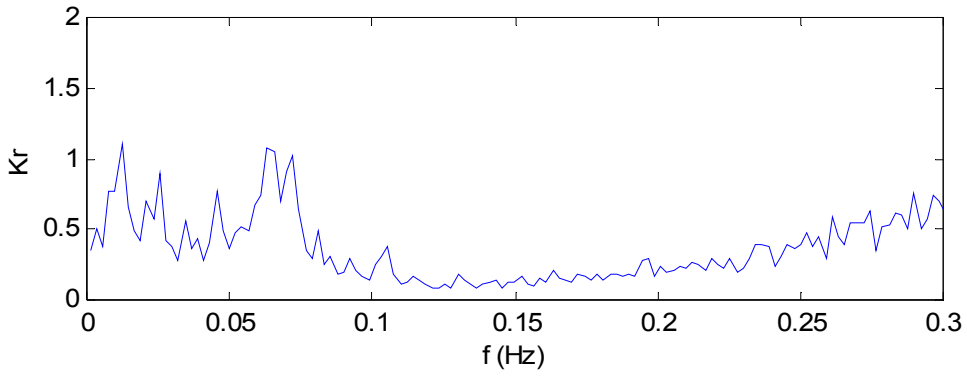

Figure F2.9 Wave reflection as function of wave frequency (condition 9).

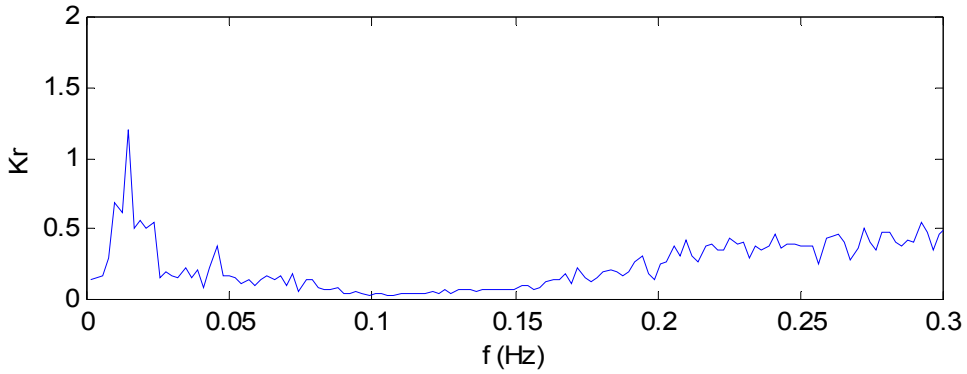

Figure F2.10 Wave reflection as function of wave frequency (condition 10).

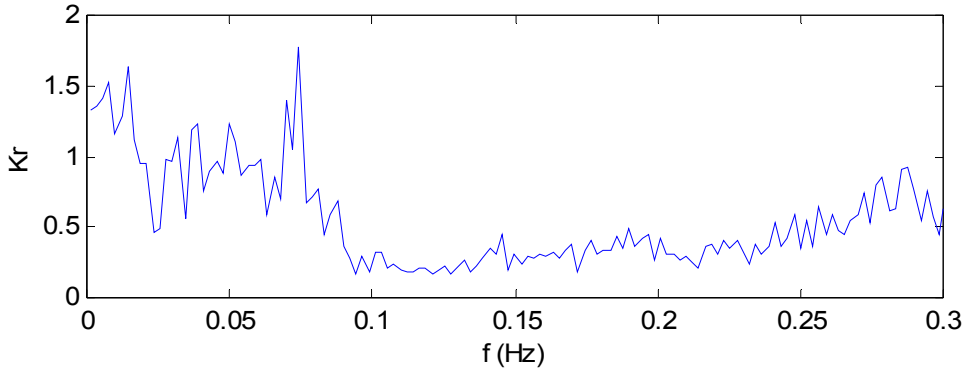

Figure F2.11 Wave reflection as function of wave frequency (condition 11).

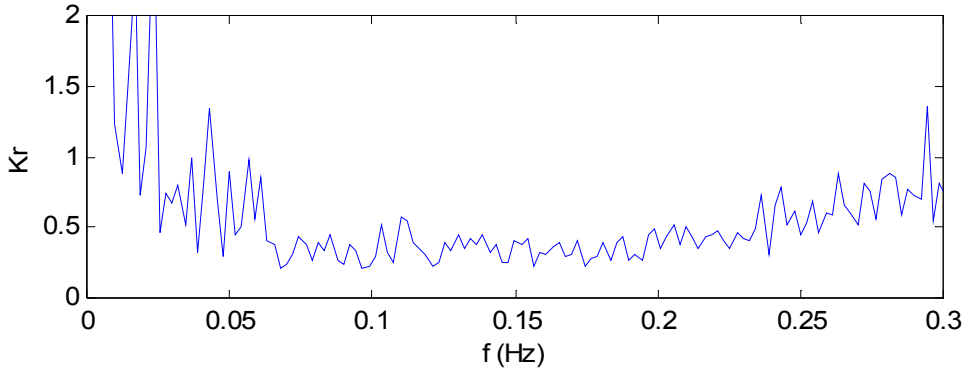

Figure F2.12 Wave reflection as function of wave frequency (condition 12).

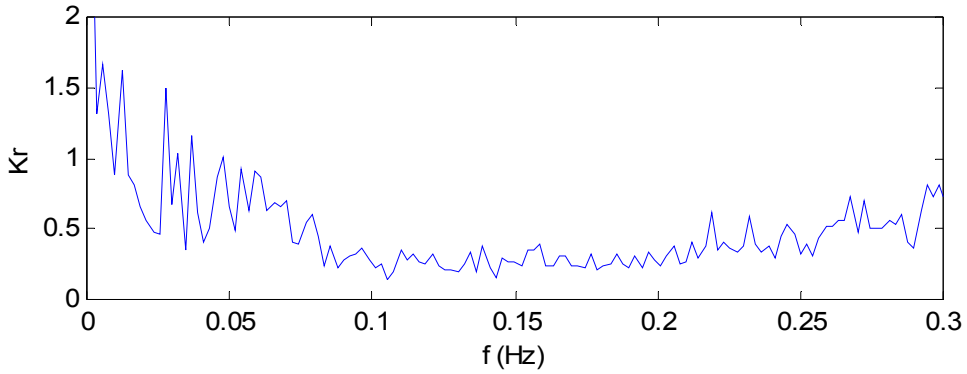

Figure F2.13 Wave reflection as function of wave frequency (condition 13).

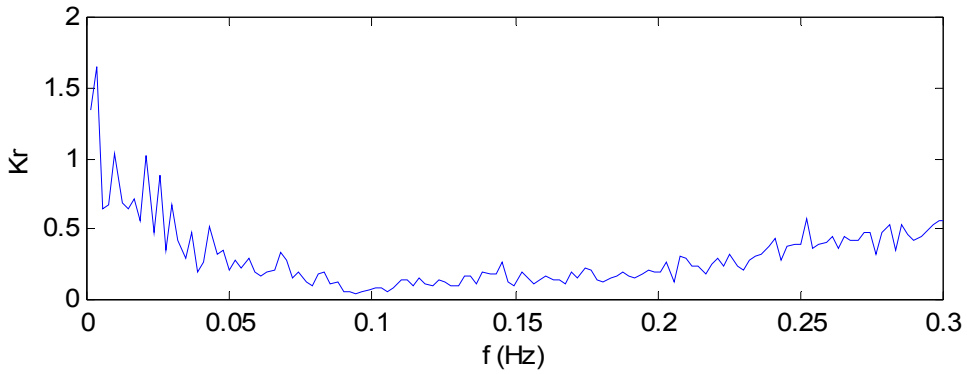

Figure F2.14 Wave reflection as function of wave frequency (condition 14).

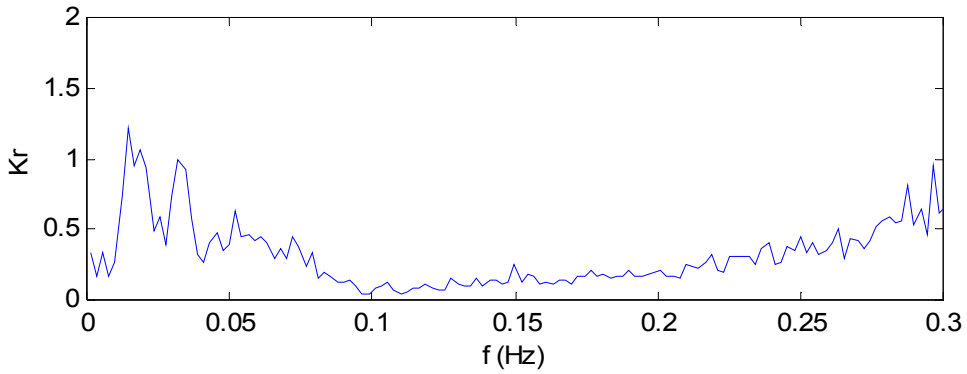

Figure F2.15 Wave reflection as function of wave frequency (condition 15).

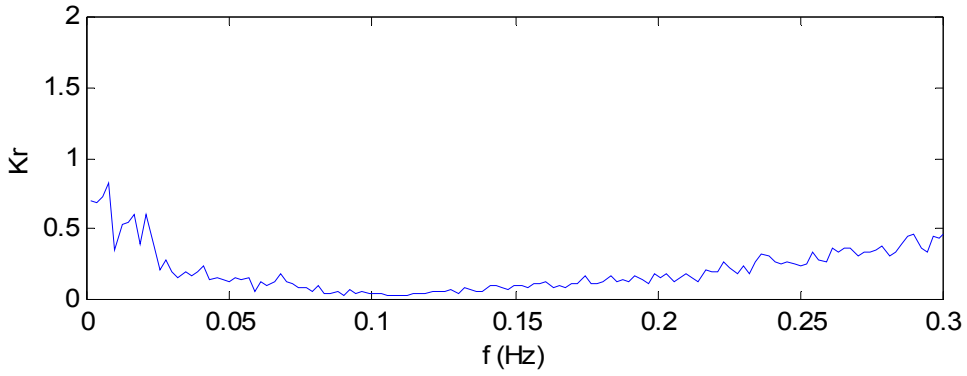

Figure F2.16 Wave reflection as function of wave frequency (condition 16).

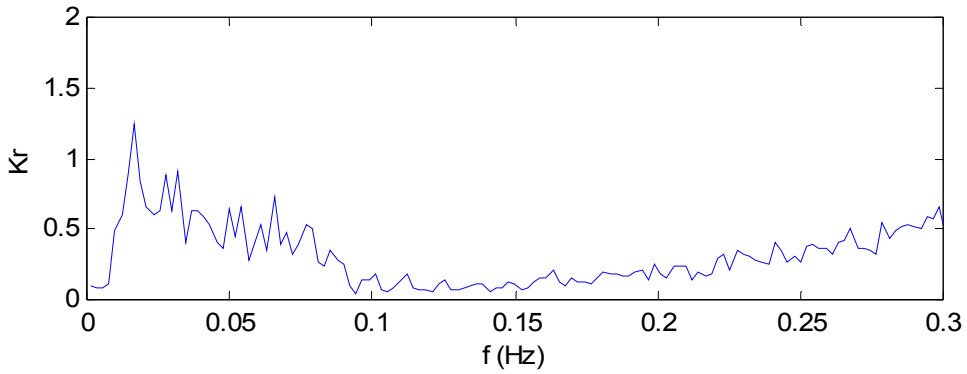

Figure F2.17 Wave reflection as function of wave frequency (condition 17).

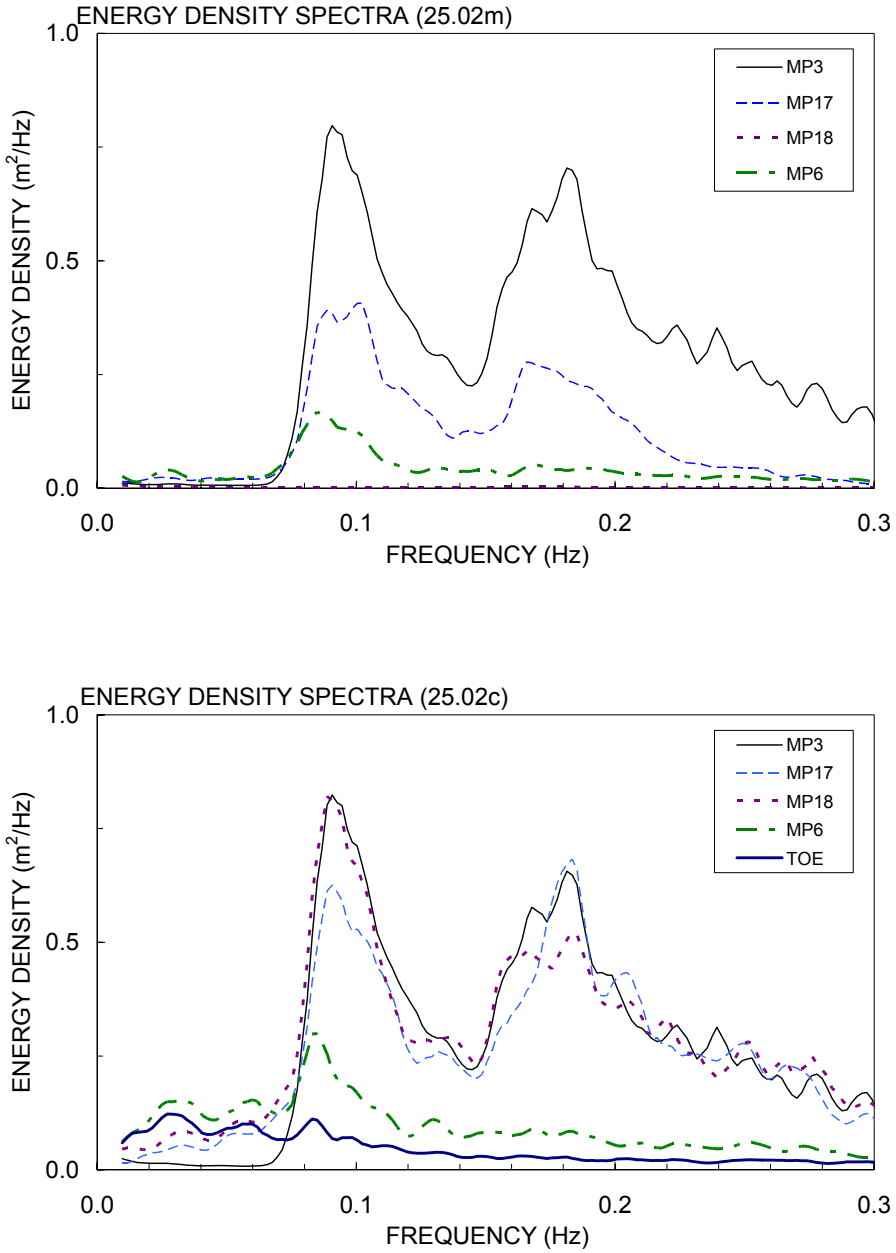

Figure F3.1 Measured (upper) and computed (lower) wave energy spectra (condition 1).

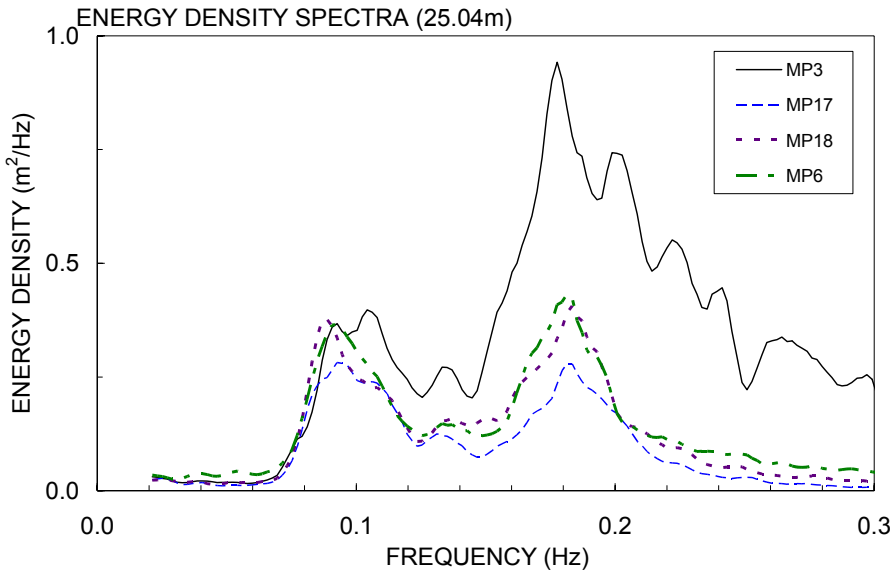

Figure F3.2 Measured wave energy spectra (condition 2).

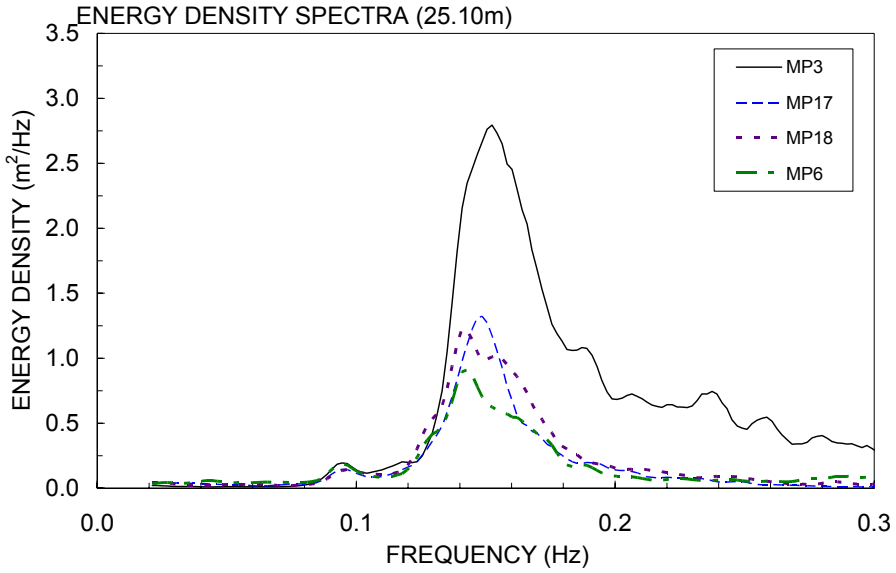

Figure F3.3 Measured wave energy spectra (condition 3).

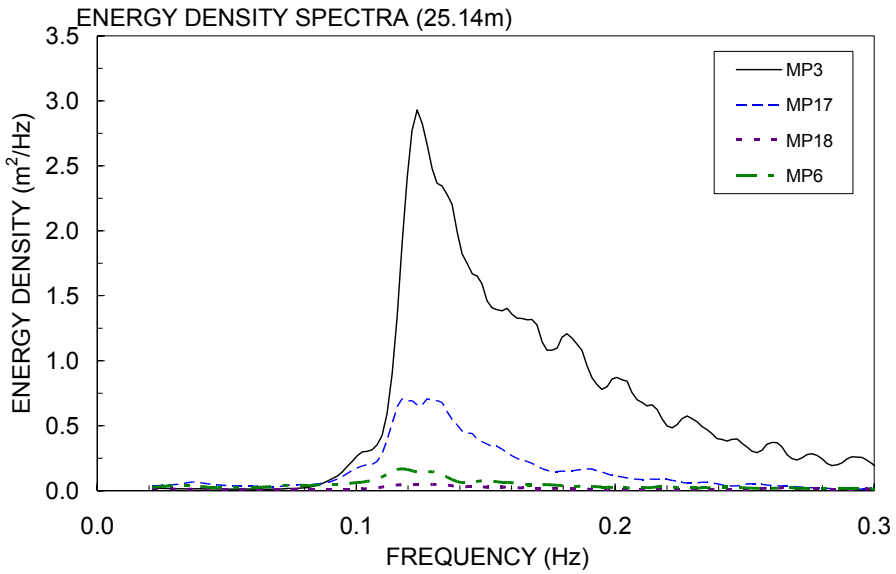

Figure F3.4 Measured wave energy spectra (condition 4).

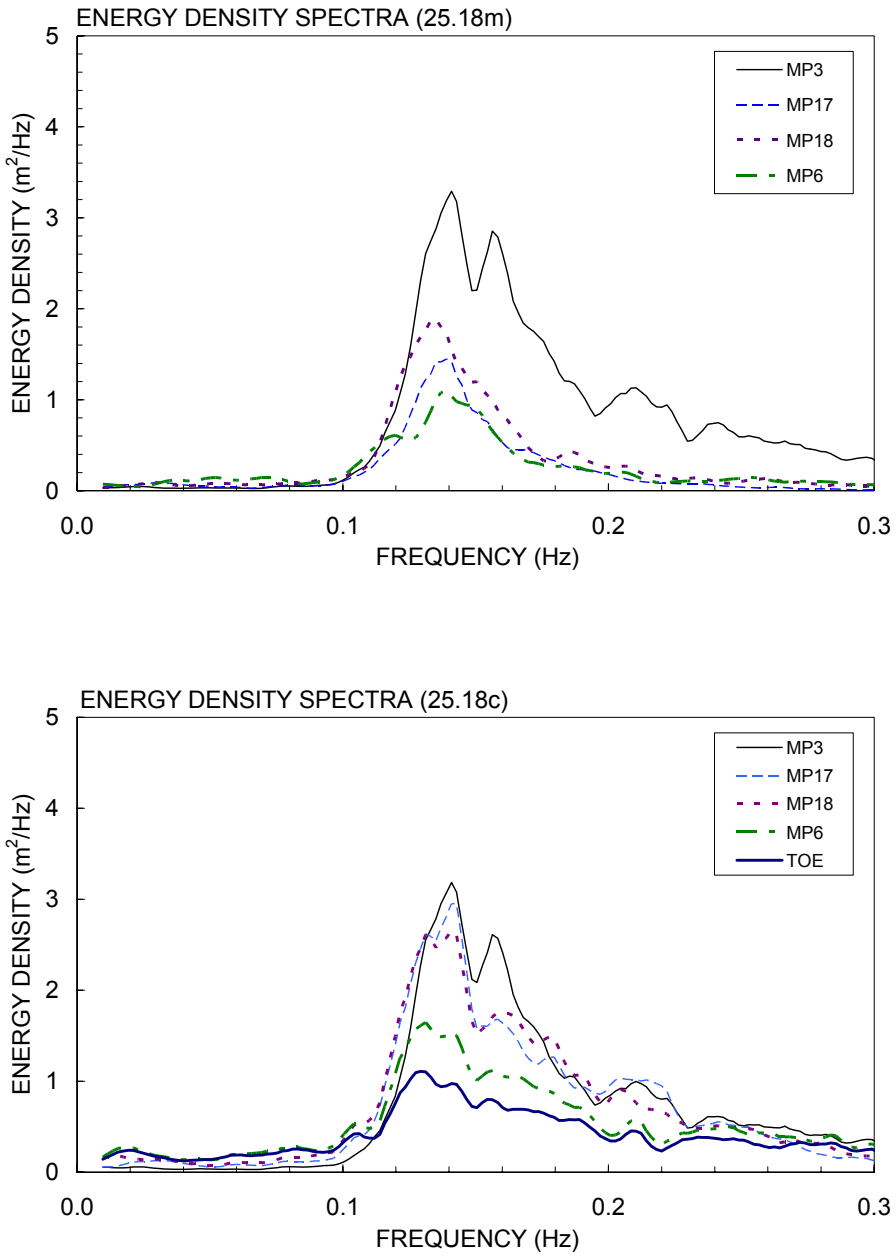

Figure F3.5 Measured (upper) and computed (lower) wave energy spectra (condition 5).

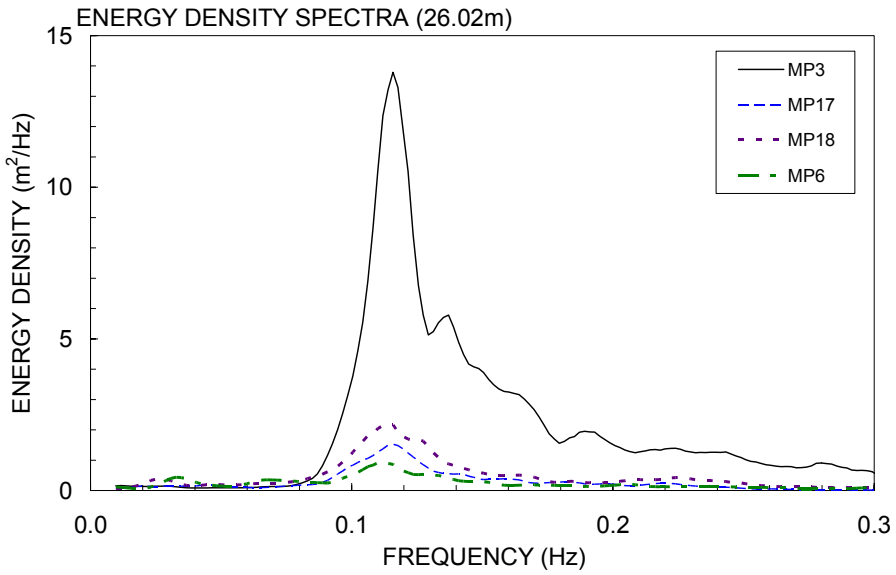

Figure F3.6 Measured wave energy spectra (condition 6).

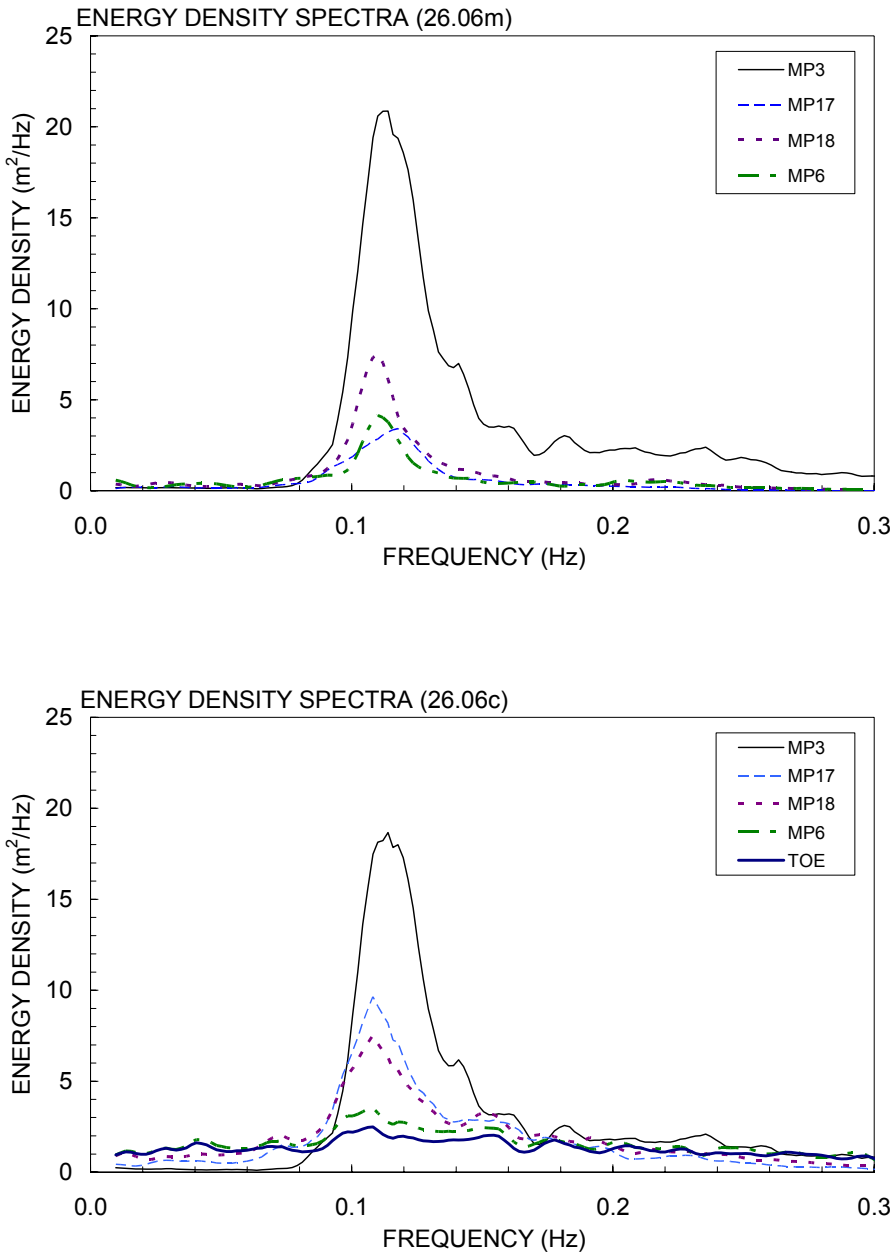

Figure F3.7 Measured (upper) and computed (lower) wave energy spectra (condition 7).

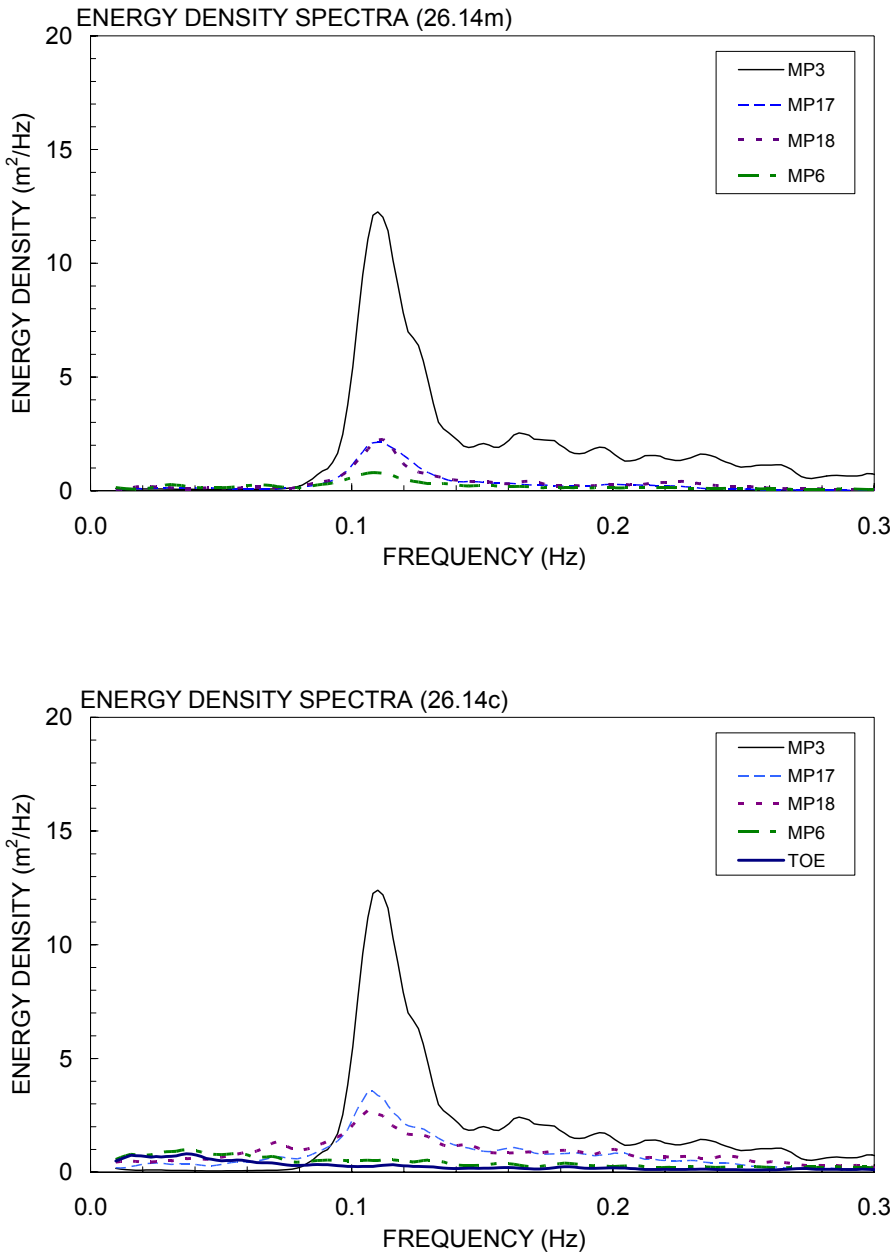

Figure F3.8 Measured (upper) and computed (lower) wave energy spectra (condition 8).

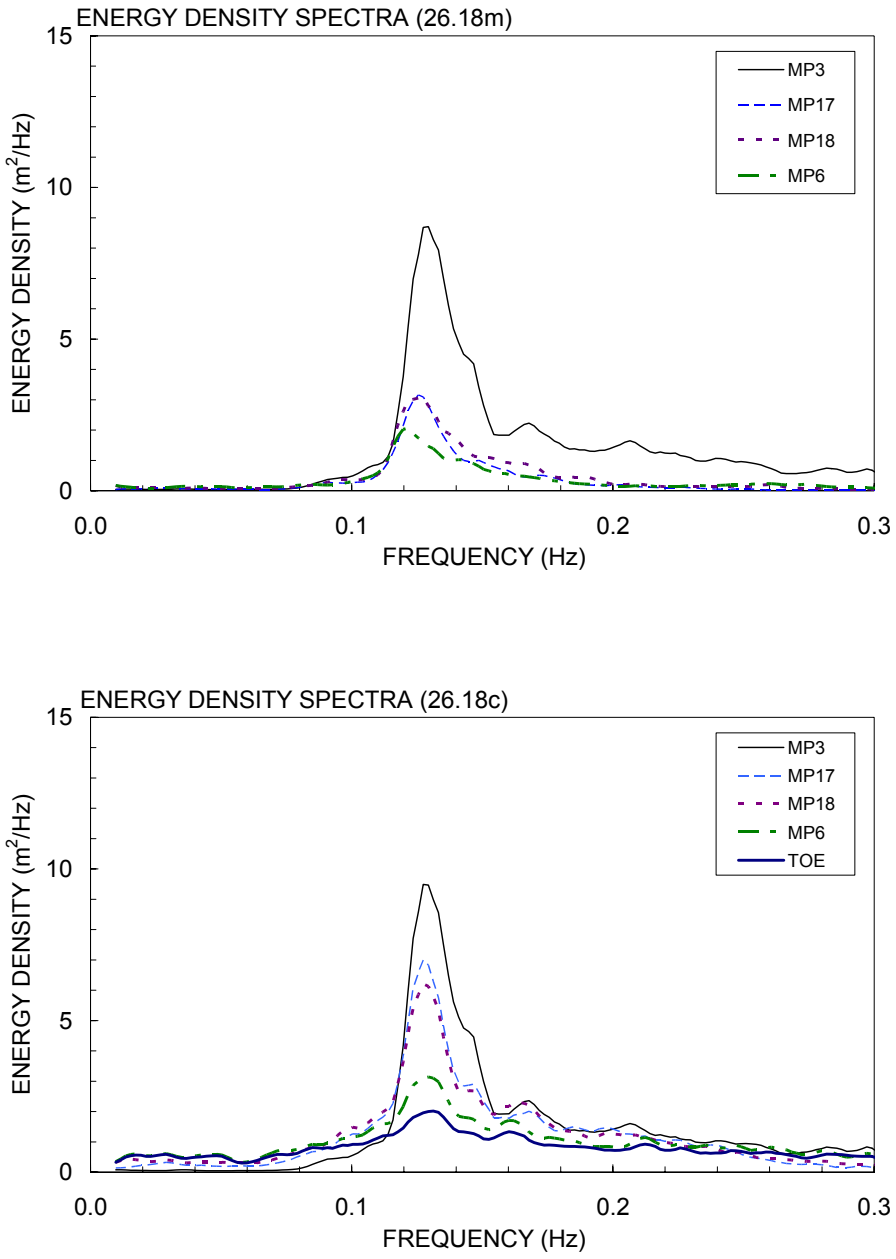

Figure F3.9 Measured (upper) and computed (lower) wave energy spectra (condition 9).

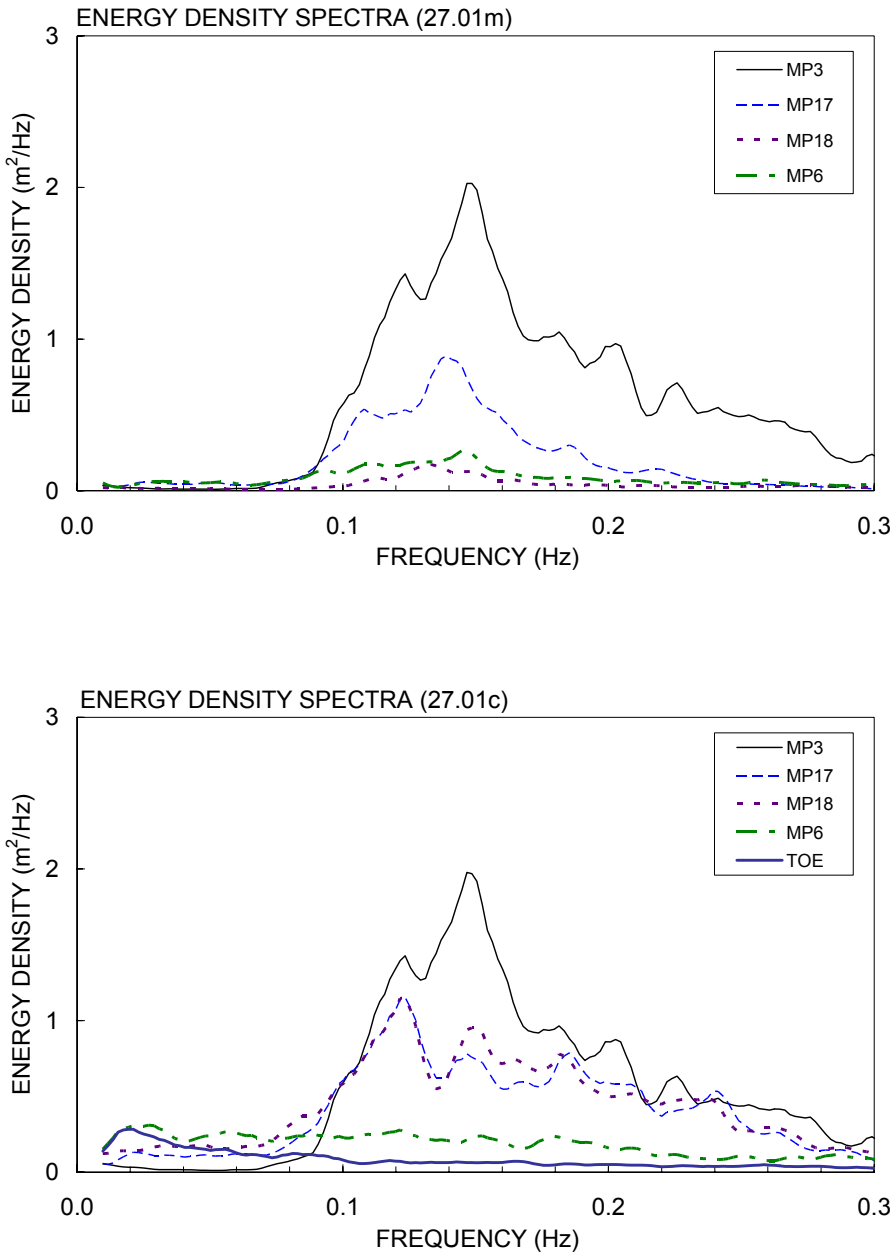

Figure F3.10 Measured (upper) and computed (lower) wave energy spectra (condition 10).

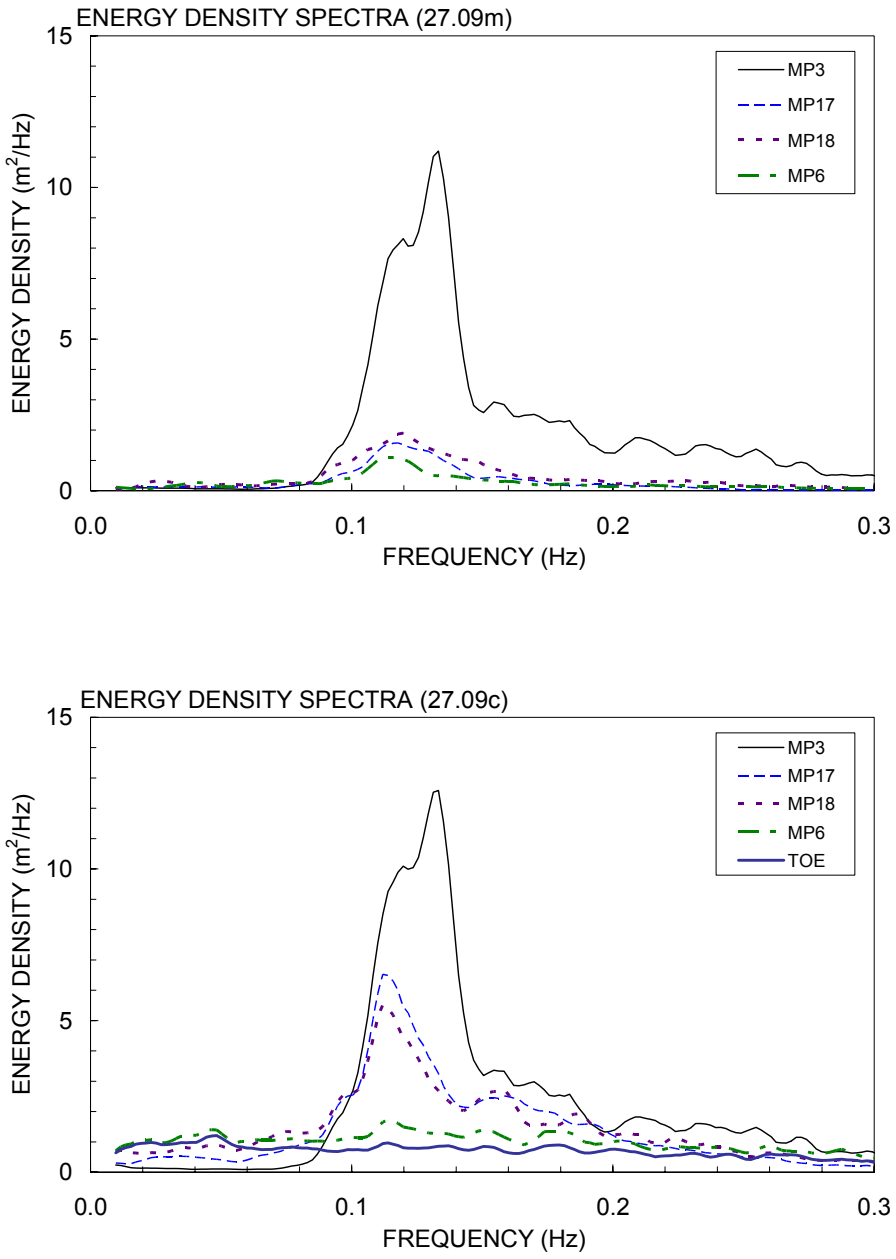

Figure F3.11 Measured (upper) and computed (lower) wave energy spectra (condition 11).

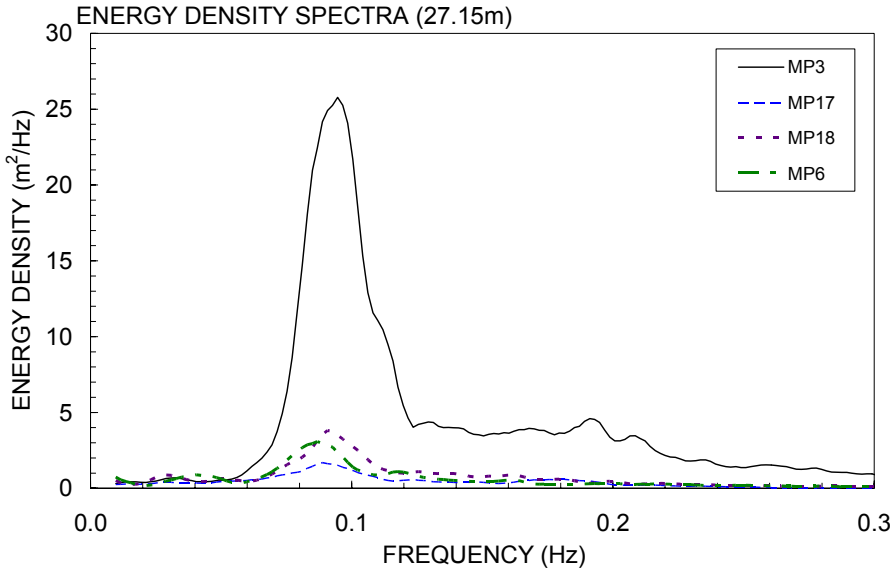

Figure F3.12 Measured wave energy spectra (condition 12).

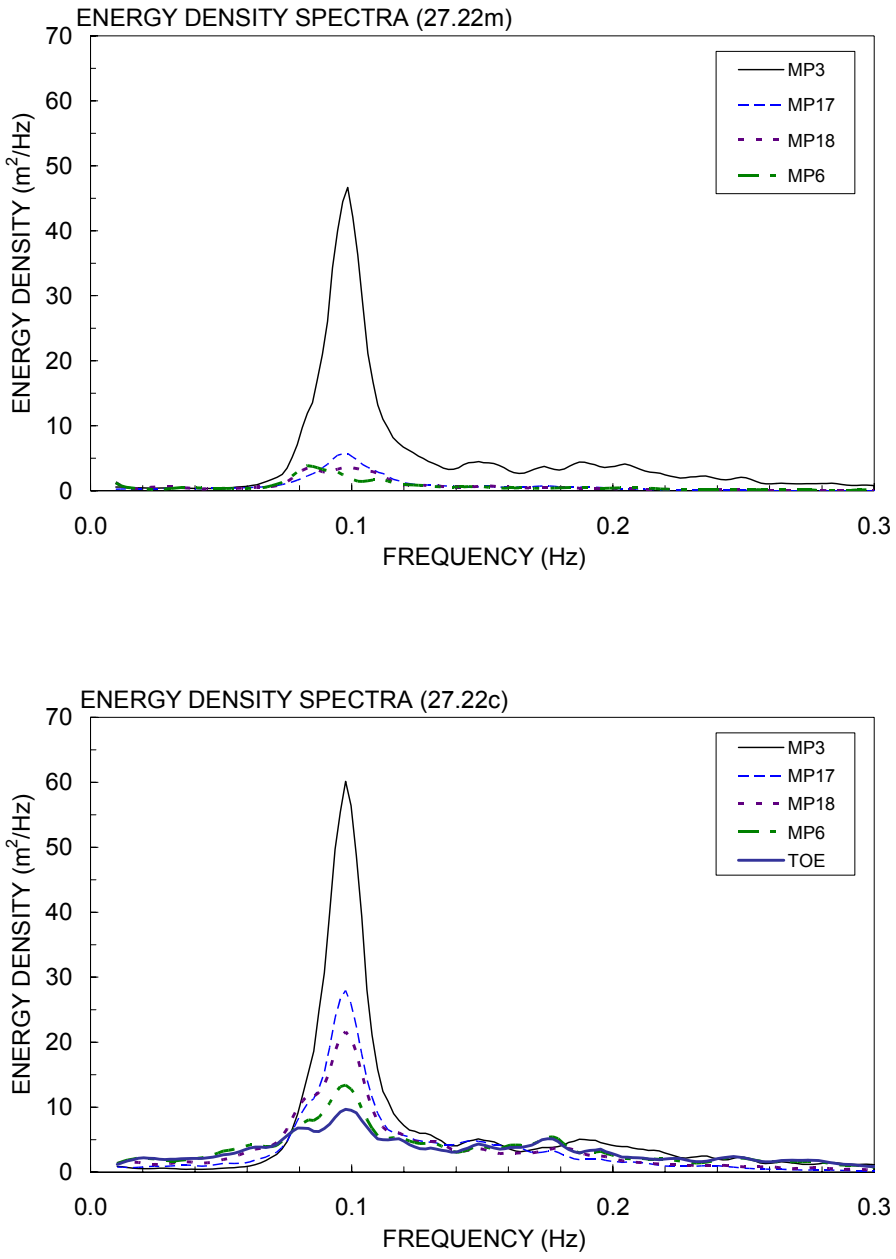

Figure F3.13 Measured (upper) and computed (lower) wave energy spectra (condition 13).

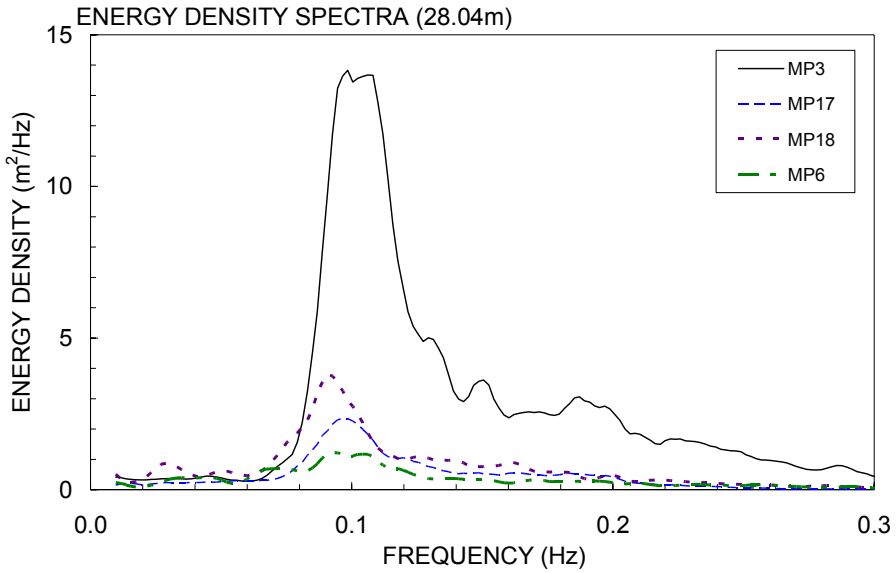

Figure F3.14 Measured wave energy spectra (condition 14).

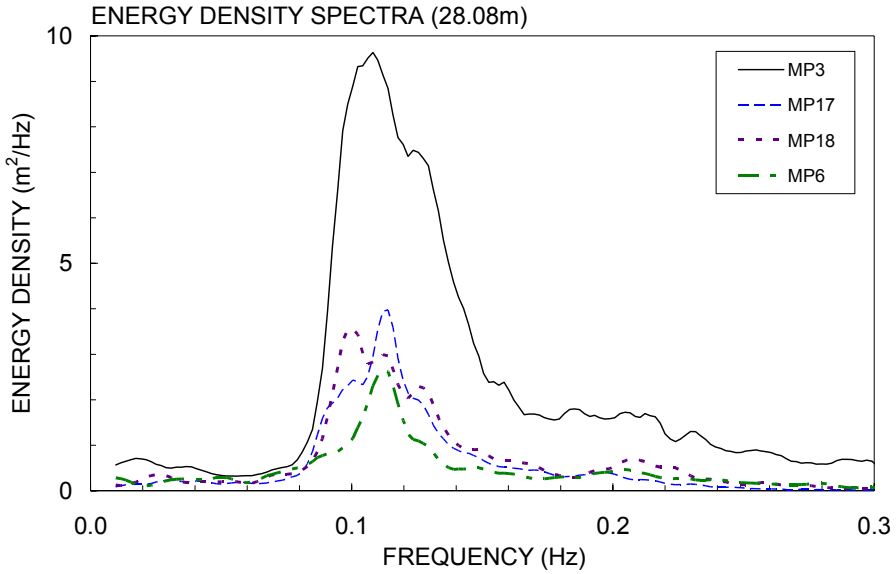

Figure F3.15 Measured wave energy spectra (condition 15).

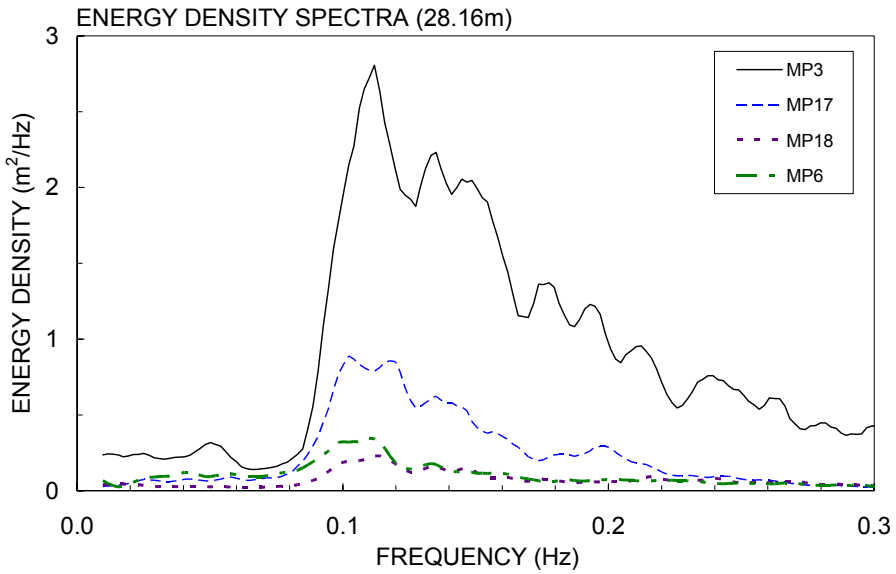

Figure F3.16 Measured wave energy spectra (condition 16).

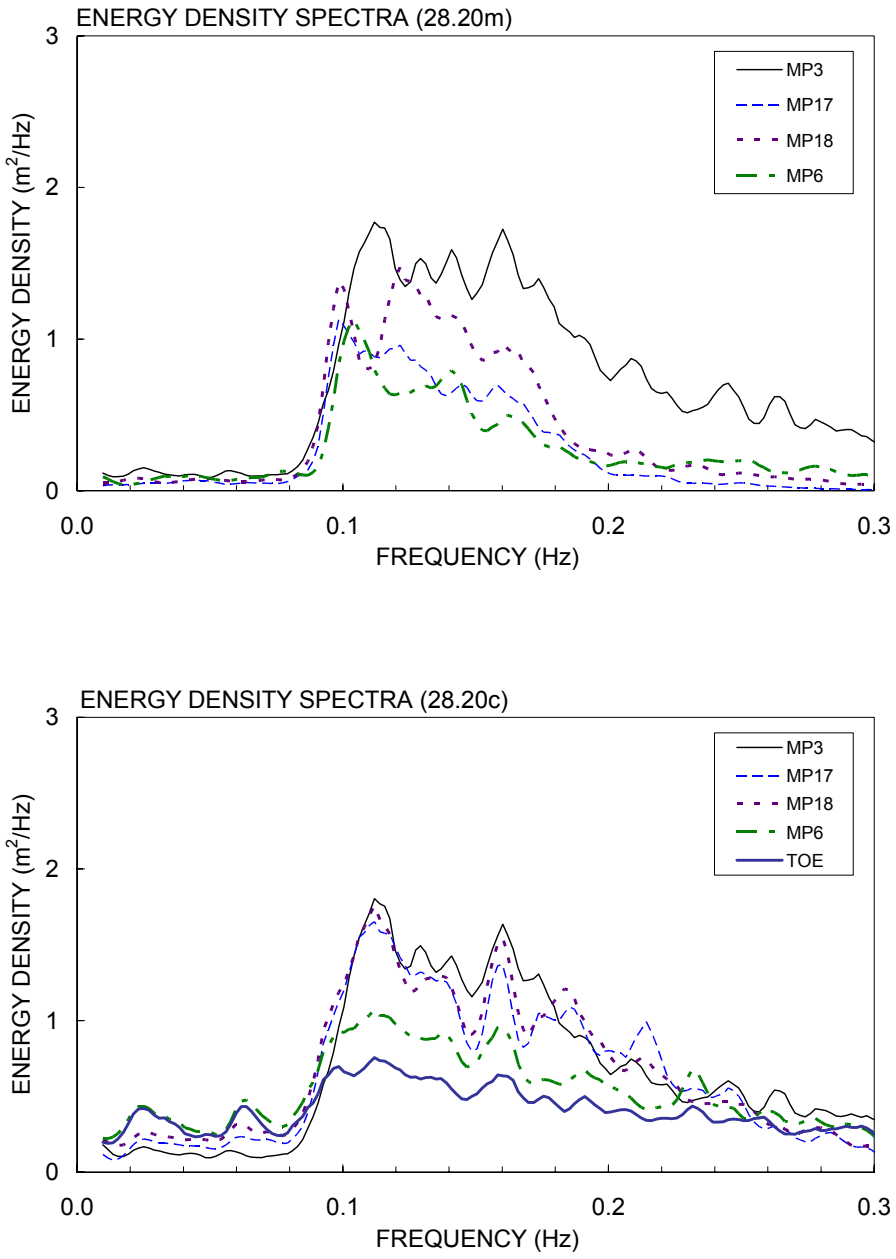

Figure F3.17 Measured (upper) and computed (lower) wave energy spectra (condition 17).